

# Basil: A Fast and Byzantine-Resilient Approach for Decentralized Training

Ahmed Roushdy Elkordy, Saurav Prakash, Salman Avestimehr

**Abstract**—Decentralized (i.e., serverless) training across edge nodes can suffer substantially from potential Byzantine nodes that can degrade the training performance. However, detection and mitigation of Byzantine behaviors in a decentralized learning setting is a daunting task, especially when the data distribution at the users is heterogeneous. As our main contribution, we propose **Basil**, a fast and computationally efficient Byzantine-robust algorithm for decentralized training systems, which leverages a novel sequential, memory-assisted and performance-based criteria for training over a logical ring while filtering the Byzantine users. In the IID dataset setting, we provide the theoretical convergence guarantees of **Basil**, demonstrating its linear convergence rate. Furthermore, for the IID setting, we experimentally demonstrate that **Basil** is robust to various Byzantine attacks, including the strong Hidden attack, while providing up to absolute  $\sim 16\%$  higher test accuracy over the state-of-the-art Byzantine-resilient decentralized learning approach. Additionally, we generalize **Basil** to the non-IID setting by proposing Anonymous Cyclic Data Sharing (ACDS), a technique that allows each node to anonymously share a random fraction of its local non-sensitive dataset (e.g., landmarks images) with all other nodes. Finally, to reduce the overall latency of **Basil** resulting from its sequential implementation over the logical ring, we propose **Basil+** that enables Byzantine-robust parallel training across groups of logical rings, and at the same time, it retains the performance gains of **Basil** due to sequential training within each group. Furthermore, we experimentally demonstrate the scalability gains of **Basil+** through different sets of experiments.

**Index Terms**—decentralized training, federated learning, Byzantine-robustness.

## I. INTRODUCTION

Thanks to the large amounts of data generated on and held by the edge devices, machine learning (ML) applications can achieve significant performance [1], [2]. However, privacy concerns and regulations [3] make it extremely difficult to pool clients' datasets for a centralized ML training procedure. As a result, distributed machine learning methods are gaining a surge of recent interests. The key underlying goal in distributed machine learning at the edge is to learn a global model using the data stored across the edge devices.

Federated learning (FL) has emerged as a promising framework [4] for distributed machine learning. In federated learning, the training process is facilitated by a central server. In an FL architecture, the task of training is federated among the clients themselves. Specifically, each participating client trains a local model based on its own (private) training dataset and shares only the trained local model with the

central entity, which appropriately aggregates the clients' local models. While the existence of the parameter server in FL is advantageous for orchestrating the training process, it brings new security and efficiency drawbacks [4], [5]. Particularly, the parameter server in FL is a single point of failure, as the entire learning process could fail when the server crashes or gets hacked. Additionally, the parameter server can become a performance bottleneck itself due to the large number of the mobile devices that need to be handled simultaneously.

Training using a decentralized setup is another approach for distributed machine learning without having to rely on a central coordinator (e.g., parameter server), thus avoiding the aforementioned limitations of FL. Instead, it only requires on-device computations on the edge nodes and peer-to-peer communications. In fact, many decentralized training algorithms have been proposed for the decentralized training setup. In particular, a class of gossip-based algorithms over random graphs has been proposed, e.g., [6]–[8], in which all the nodes participate in each training round. During training, each node maintains a local model and communicates with others over a graph-based decentralized network. More specifically, every node updates its local model using its local dataset, as well as the models received from the nodes in its neighborhood. For example, a simple aggregation rule at each node is to average the locally updated model with the models from the neighboring nodes. Thus, each node performs both model training and model aggregation.

Although decentralized training provides many benefits, its decentralized nature makes it vulnerable to performance degradation due to system failures, malicious nodes, and data heterogeneity [4]. Specifically, one of the key challenges in decentralized training is the presence of different threats that can alter the learning process, such as the software/hardware errors and adversarial attacks. Particularly, some clients can become faulty due to software bugs, hardware components which may behave arbitrarily, or even get hacked during training, sending arbitrary or malicious values to other clients, thus severely degrading the overall convergence performance. Such faults, where client nodes arbitrarily deviate from the agreed-upon protocol, are called Byzantine faults [9]. To mitigate Byzantine nodes in a graph-based decentralized setup where nodes are randomly connected to each other, some Byzantine-robust optimization algorithms have been introduced recently, e.g., [10], [11]. In these algorithms, each node combines the set of models received from its neighbors by using robust aggregation rules, to ensure that the training is not impacted by the Byzantine nodes. However, to the best of our knowledge, none of these algorithms have considered the scenario when

The authors are with the Electrical Engineering Department, University of Southern California, Los Angeles, CA 90089, USA (e-mail: aelkordy@usc.edu sauravpr@usc.edu, avestimehr@ee.usc.edu).

the data distribution at the nodes is heterogeneous. Data heterogeneity makes the detection of Byzantine nodes a daunting task, since it becomes unclear whether the model drift can be attributed to a Byzantine node, or to the very heterogeneous nature of the data. Even in the absence of Byzantine nodes, data heterogeneity can degrade the convergence rate [4].

The limited computation and communication resources of edge devices (e.g., IoT devices) are another important consideration in the decentralized training setting. In fact, the resources at the edge devices are considered as a critical bottleneck for performing distributed training for large models [1], [4]. In prior Byzantine-robust decentralized algorithms (e.g., [10], [11]), which are based on parallel training over a random graph, all nodes need to be always active and perform training during the entire training process. Therefore, they might not be suitable for the resource constrained edge devices, as the parallel training nature of their algorithms requires them to be perpetually active which could drain their resources. In contrast to parallel training over a random graph, our work takes the view that sequential training over a logical ring is better suited for decentralized training in resource constrained edge setting. Specifically, sequential training over a logical ring allows each node to become active and perform model training *only* when it receives the model from its counterclockwise neighbor. Since nodes need not be active during the whole training time, the sequential training nature makes it suitable for IoT devices with limited computational resources.

### A. Contributions

To overcome the aforementioned limitations of prior graph-based Byzantine-robust algorithms, we propose *Basil*, an efficient Byzantine mitigation algorithm, that achieves Byzantine robustness in a decentralized setting by leveraging the sequential training over a logical ring. To highlight some of the benefits of *Basil*, Fig. 1(a) illustrates a sample result that demonstrates the performance gains and the cost reduction compared to the state-of-the-art Byzantine-robust algorithm UBAR that leverages the parallel training over a graph-based setting. We observe that *Basil* retains a higher accuracy than UBAR with an absolute value of  $\sim 16\%$ . Additionally, we note that while UBAR achieves its highest accuracy in  $\sim 500$  rounds, *Basil* achieves UBAR’s highest accuracy in just  $\sim 100$  rounds. This implies that for achieving UBAR’s highest accuracy, each client in *Basil* uses  $5\times$  lesser computation and communication resources compared to that in UBAR confirming the gain attained from the sequential training nature of *Basil*.

In the following, we further highlight the key aspects and performance gains of *Basil*:

- In *Basil*, the defense technique to filter out Byzantine nodes is a performance-based strategy, wherein each node evaluates a received set of models from its counterclockwise neighbors by using its own local dataset to select the best candidate.
- We theoretically show that *Basil* for convex loss functions in the IID data setting has a linear convergence

rate with respect to the product of the number of benign nodes and the total number of training rounds over the ring. Thus, our theoretical result demonstrates scalable performance for *Basil* with respect to the number of nodes.

- We empirically demonstrate the superior performance of *Basil* compared to UBAR, the state-of-the-art Byzantine-resilient decentralized learning algorithm over graph, under different Byzantine attacks in the IID setting. Additionally, we study the performance of *Basil* and UBAR with respect to the wall-clock time in Appendix H showing that the training time for *Basil* is comparable to UBAR.
- For extending the superior benefits of *Basil* to the scenario when data distribution is non-IID across devices, we propose Anonymous Cyclic Data Sharing (ACDS) to be applied on top of *Basil*. To the best of our knowledge, no prior decentralized Byzantine-robust algorithm has considered the scenario when the data distribution at the nodes is non-IID. ACDS allows each node to share a random fraction of its local non-sensitive dataset (e.g., landmarks images captured during tours) with all other nodes, while guaranteeing anonymity of the node identity. As highlighted in Section I-B, there are multiple real-world use cases where anonymous data sharing is sufficient to meet the privacy concerns of the users.
- We experimentally demonstrate that using ACDS with only 5% data sharing on top of *Basil* provides resiliency to Byzantine behaviors, unlike UBAR which diverges in the non-IID setting (Fig. 1(c)).
- As the number of participating nodes in *Basil* scales, the increase in the overall latency of sequential training over the logical ring topology may limit the practicality of implementing *Basil*. Therefore, we propose a parallel extension of *Basil*, named *Basil+*, that provides further scalability by enabling Byzantine-robust parallel training across groups of logical rings, while retaining the performance gains of *Basil* through sequential training within each group.

### B. Related Works

Many Byzantine-robust strategies have been proposed recently for the distributed training setup (federated learning) where there is a central server to orchestrate the training process [12]–[22]. These Byzantine-robust optimization algorithms combine the gradients received by all workers using robust aggregation rules, to ensure that training is not impacted by malicious nodes. Some of these strategies [15]–[19] are based on distance-based approaches, while some others are based on performance-based criteria [12]–[14], [21]. The key idea in distance-based defense solutions is to filter the updates that are far from the average of the updates from the benign nodes. It has been shown that distance-based solutions are vulnerable to the sophisticated Hidden attack proposed in [23]. In this attack, Byzantine nodes could create gradients that are malicious but indistinguishable from benign gradients in distance. On the other hand, performance-based filtering

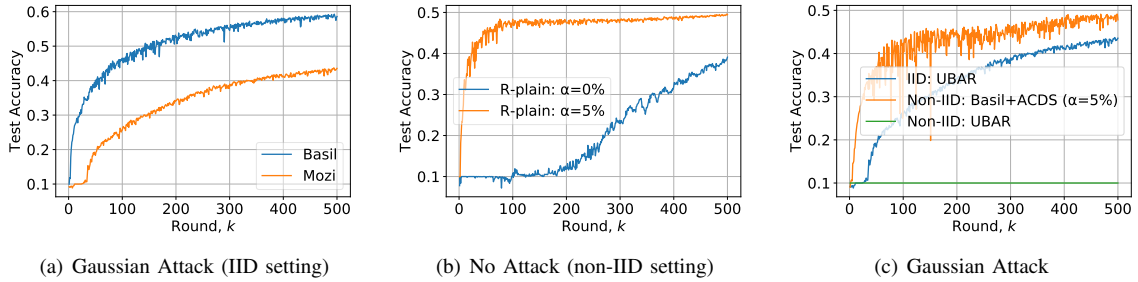


Fig. 1. A highlight of the performance benefits of `Basil`, compared with state-of-the-art (UBAR) [10], for CIFAR10 under different settings: In Fig. 1(a), we can see the superior performance of `Basil` over UBAR with  $\sim 16\%$  improvement of the test accuracy under Gaussian attack in the IID setting. Fig. 1(b) demonstrates that the test accuracy in the non-IID setting by using sequential training over the ring topology can be increased by up to  $\sim 10\%$  in the absence of Byzantine nodes, when each node shares only 5% of its local data anonymously with other nodes. Fig. 1(c) shows that ACDS on the top of `Basil` not only provides Byzantine robustness to Gaussian attack in the non-IID setting, but also gives higher performance than UBAR in the IID setting. Furthermore, UBAR for the non-IID setting completely fails in the presence of this attack. For further details, please refer to Section VI.

strategies rely on having some auxiliary dataset at the server to evaluate the model received from each node.

Compared to the large number of Byzantine-robust training algorithms for distributed training in the presence of a central server, there have been only a few recent works on Byzantine resiliency in the decentralized training setup with no central coordinator. In particular, to address Byzantine failures in a decentralized training setup over a random graph under the scenario when the data distribution at the nodes is IID, the authors in [11] propose using a trimmed mean distance-based approach called BRIDGE to mitigate Byzantine nodes. However, the authors in [10] demonstrate that BRIDGE is defeated by the hidden attack proposed in [23]. To solve the limitations of the distance-based approaches in the decentralized setup, [10] proposes an algorithm called UBAR in which a combination of performance-based and distance-based stages are used to mitigate the Byzantine nodes, where the performance-based stage at a particular node leverages only its local dataset. As demonstrated numerically in [10], the combination of these two strategies allows UBAR to defeat the Byzantine attack proposed in [23]. However, UBAR is not suitable for the training over resource-constrained edge devices, as the training is carried out in parallel and nodes remain active all the time. In contrast, `Basil` is a fast and computationally efficient Byzantine-robust algorithm, which leverages a novel sequential, memory-assisted and performance-based criteria for training over a logical ring while filtering the Byzantine users.

Data heterogeneity in the decentralized setting has been studied in some recent works (e.g., [24]) in the absence of Byzantine nodes. In particular, the authors of TornadoAggregate [24] propose to cluster users into groups based on an algorithm called Group-BY-IID and CLUSTER where both use EMD (earth mover distance) that can approximately model the learning divergences between the models to complete the grouping. However, EMD function relies on having a publicly shared data at each node which can be collected similarly as in [25]. In particular, to improve training on non-IID data in federated learning, [25] proposed sharing of small portions of users' data with the server. The parameter server pools the received subsets of data thus creating a small subset of the data distributed at the clients, which is then globally shared

between all the nodes to make the data distribution close to IID. However, the aforementioned data sharing approach is considered insecure in scenarios where users are fine with sharing some of their datasets with each other but want to keep their identities anonymous, i.e., data shares should not reveal who the data owners are.

There are multiple real-world use cases where anonymous data sharing is sufficient for privacy concerns. For example, mobile users maybe fine with sharing some of their own text data, which does not contain any personal and sensitive information with others, as long as their personal identities remain anonymous. Another example is sharing of some non-private data (such as landmarks images) collected by a person with others. In this scenario, although data itself is not generated at the users, revealing the identity of the users can potentially leak private information such as personal interests, location, or travel history. Our proposed ACDS strategy is suitable for such scenarios as it guarantees that the owner identity of the shared data points are kept hidden.

As a final remark, we point out that for anonymous data sharing, [26] proposed an approach which is based on utilizing a secure sum operation along with anonymous ID assignment (AIDA). This involves computational operations at the nodes such as polynomial evaluations and some arithmetic operations such as modular operations. Thus, this algorithm may fail in the presence of Byzantine faults arising during these computations. Particularly, computation errors or software bugs can be present during the AIDA algorithm thus leading to the failure of anonymous ID assignment, or during the secure sum algorithm which can lead to distortion of the shared data.

## II. PROBLEM STATEMENT

We formally define the decentralized learning system in the presence of Byzantine faults.

### A. Decentralized System Model

We consider a decentralized learning setting in which a set  $\mathcal{N} = \{1, \dots, N\}$  of  $|\mathcal{N}| = N$  nodes collaboratively train a machine learning (ML) model  $\mathbf{x} \in \mathbb{R}^d$ , where  $d$  is the model size, based on all the training data samples  $\cup_{n \in \mathcal{N}} \mathcal{Z}_n$  that are

generated and stored at these distributed nodes, where the size of each local dataset is  $|\mathcal{Z}_i| = D_i$  data points.

In this work, we are motivated by the edge IoT setting, where users want to collaboratively train an ML model, in the absence of a centralized parameter server. The communication in this setting leverages the underlay communication fabric of the internet that connects any pair of nodes directly via overlay communication protocols. Specifically, we assume that there is no central parameter server, and consider the setup where the training process is carried out in a sequential fashion over a clockwise directed ring. Each node in this ring topology takes part in the training process when it receives the model from the previous counterclockwise node. In Section III-A, we propose a method in which nodes can consensually agree on a random ordering on a logical ring at the beginning of the training process, so that each node knows the logical ring positions of the other nodes. Therefore, without loss of generality, we assume for notation simplification that the indices of nodes in the ring are arranged in ascending order starting from node 1. In this setup, each node can send its model update to any set of users in the network.

In this decentralized setting, an unknown  $\beta$ -proportion of nodes can be Byzantine, where  $\beta \in (0, 1)$ , meaning they can send arbitrary and possibly malicious results to the other nodes. We denote  $\mathcal{R}$  (with cardinality  $|\mathcal{R}| = r$ ) and  $\mathcal{B}$  (with cardinality  $|\mathcal{B}| = b$ ) as the sets of benign nodes and Byzantine nodes, respectively. Furthermore, Byzantine nodes are uniformly distributed over the ring due to consensus-based random order agreement. Finally, we assume nodes can authenticate the source of a message, so no Byzantine node can forge its identity or create multiple fake ones [27].

### B. Model Training

Each node in the set  $\mathcal{R}$  of benign nodes uses its own dataset to collaboratively train a shared model by solving the following optimization problem in the presence of Byzantine nodes:

$$\mathbf{x}^* = \arg \min_{\mathbf{x} \in \mathbb{R}^d} \left[ f(\mathbf{x}) := \frac{1}{r} \sum_{i=1}^r f_i(\mathbf{x}) \right], \quad (1)$$

where  $\mathbf{x}$  is the optimization variable, and  $f_i(\mathbf{x})$  is the expected loss function of node  $i$  such that  $f_i(\mathbf{x}) = \mathbb{E}_{\zeta_i \sim \mathcal{P}_i} [l_i(\mathbf{x}, \zeta_i)]$ . Here,  $l_i(\mathbf{x}, \zeta_i) \in \mathbb{R}$  denotes the loss function for model parameter  $\mathbf{x} \in \mathbb{R}^d$  for a given realization  $\zeta_i$ , which is generated from a distribution  $\mathcal{P}_i$ .

The general update rule in this decentralized setting is given as follows. At the  $k$ -th round, the current active node  $i$  updates the global model according to:

$$\mathbf{x}_k^{(i)} = \bar{\mathbf{x}}_k^{(i)} - \eta_k^{(i)} g_i(\bar{\mathbf{x}}_k^{(i)}), \quad (2)$$

where  $\bar{\mathbf{x}}_k^{(i)} = \mathcal{A}(\mathbf{x}_v^{(j)}, j \in \mathcal{N}, v = 1, \dots, k)$  is the selected model by node  $i$  according to the underlying aggregation rule  $\mathcal{A}$ ,  $g(\bar{\mathbf{x}}_k^{(i)})$  is the stochastic gradient computed by node  $i$  by using a random sample from its local dataset  $\mathcal{Z}_i$ , and  $\eta_k^{(i)}$  is the learning rate in round  $k$  used by node  $i$ .

**Threat model:** Byzantine node  $i \in \mathcal{B}$  could send faulty or malicious update  $\mathbf{x}_k^{(i)} = *$ , where “\*” denotes that  $\mathbf{x}_k^{(i)}$  can

be an arbitrary vector in  $\mathbb{R}^d$ . Furthermore, Byzantine nodes cannot forge their identities or create multiple fake ones. This assumption has been used in different prior works (e.g., [27]).

Our goal is to design an algorithm for the decentralized training setup discussed earlier, while mitigating the impact of the Byzantine nodes. Towards achieving this goal, we propose `Basil` that is described next.

## III. THE PROPOSED BASIL ALGORITHM

Now, we describe `Basil`, our proposed approach for mitigating both malicious updates and faulty updates in the IID setting, where the local dataset  $\mathcal{Z}_i$  at node  $i$  consists of IID data samples from a distribution  $\mathcal{P}_i$ , where  $\mathcal{P}_i = \mathcal{P}$  for  $i \in \mathcal{N}$ , and characterize the complexity of `Basil`. Note that, in Section IV, we extend `Basil` to the non-IID setting by integrating it to our proposed Anonymous Cyclic Data Sharing scheme.

### A. Basil for IID Setting

Our proposed `Basil` algorithm that is given in Algorithm 1 consists of two phases; initialization phase and training phase which are described below.

**Phase 1: Order Agreement over the Logical Ring.** Before the training starts, nodes consensually agree on their order on the ring by using the following simple steps. 1) All users first share their IDs with each other, and we assume WLOG that nodes’ IDs can be arranged in ascending order. 2) Each node locally generates the order permutation for the users’ IDs by using a pseudo random number generator (PRNG) initialized via a common seed (e.g.,  $N$ ). This ensures that all nodes will generate the same IDs’ order for the ring.

**Phase 2: Robust Training.** As illustrated in Fig. 2, `Basil` leverages sequential training over the logical ring to mitigate the effect of Byzantine nodes. At a high level, in the  $k$ -th round, the current active node carries out the model update step in (2), and then multicasts its updated model to the next  $S = b + 1$  clockwise nodes, where  $b$  is the worst case number of Byzantine nodes. We note that multicasting each model to the next  $b + 1$  neighbors is crucial to make sure that the benign subgraph, which is generated by excluding the Byzantine nodes, is connected. Connectivity of the benign subgraph is important as it ensures that each benign node can still receive information from a few other non-faulty nodes, i.e., the good updates can successfully propagate between the benign nodes. Even in the scenario where all Byzantine nodes come in a row, multicasting each updated model to the next  $S$  clockwise neighbors allows the connectivity of benign nodes.

We now describe how the aggregation rule  $\mathcal{A}_{\text{Basil}}$  in `Basil`, that node  $i$  implements for obtaining the model  $\bar{\mathbf{x}}_k^{(i)}$  for carrying out the update in (2), works. Node  $i$  stores the  $S$  latest models from its previous  $S$  counterclockwise neighbors. As highlighted above, the reason for storing  $S$  models is to make sure that each stored set of models at node  $i$  contains at least one good model. When node  $i$  is active, it implements our proposed performance-based criteria to pick the best model out of its  $S$  stored models. In the following, we formally define our model selection criteria:

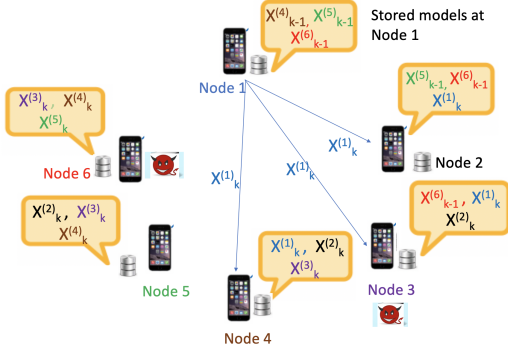


Fig. 2. Basil with  $N = 6$  nodes, where node 3 and node 6 are Byzantine nodes. Node 1, the current active benign node in the  $k$ -th round, selects one model out of its stored 3 models which gives the lowest loss when it is evaluated on a mini-batch from its local dataset  $\mathcal{Z}_1$ . After that, node 1 updates the selected model by using the same mini-batch according to (2) before multicasting it to the next 3 clockwise neighbors.

*Definition 1: (Basil Aggregation Rule)* In the  $k$ -th round over the ring, let  $\mathcal{N}_k^i = \{\mathbf{y}_1, \dots, \mathbf{y}_S\}$  be the set of  $S$  latest models from the  $S$  counterclockwise neighbors of node  $i$ . We define  $\zeta_i$  to be a random sample from the local dataset  $\mathcal{Z}_i$ , and let  $l_i(\mathbf{y}_j) = l_i(\mathbf{y}_j, \zeta_i)$  to be the loss function of node  $i$  evaluated on the model  $\mathbf{y}_j \in \mathcal{N}_k^i$ , by using a random sample  $\zeta_i$ . The proposed Basil aggregation rule is defined as

$$\bar{\mathbf{x}}_k^{(i)} = \mathcal{A}_{\text{Basil}}(\mathcal{N}_k^i) = \arg \min_{\mathbf{y} \in \mathcal{N}_k^i} \mathbb{E}[l_i(\mathbf{y}, \zeta_i)]. \quad (3)$$

In practice, node  $i$  can sample a mini-batch from its dataset and leverage it as validation data to test the performance (i.e., loss function value) of each model of the neighboring  $S$  models, and set  $\bar{\mathbf{x}}_k^{(i)}$  to be the model with the lowest loss among the  $S$  stored models. As demonstrated in our experiments in Section VI, this practical mini-batch implementation of the Basil criteria in Definition 1 is sufficient to mitigate Byzantine nodes in the network, while achieving superior performance over state-of-the-art.

In the following, we characterize the communication, computation, and storage costs of Basil.

**Proposition 1.** *The communication, computation, and storage complexities of Basil algorithm are all  $\mathcal{O}(Sd)$  for each node at each iteration, where  $d$  is the model size.*

The complexity of prior graph-based Byzantine-robust decentralized algorithms UBAR [10] and Bridge [11] is  $\mathcal{O}(H_i d)$ , where  $H_i$  is the number of neighbours (e.g., connectivity parameter) of node  $i$  on the graph. So we conclude that Basil maintains the same per round complexity as Bridge and UBAR, but with higher performance as we will show in Section VI.

The costs in Proposition 1 can be reduced by relaxing the connectivity parameter  $S$  to  $S < b + 1$  while guaranteeing the success of Basil (benign subgraph connectivity) with high probability, as formally presented in the following.

**Proposition 2.** *The number of models that each benign node needs to receive, store and evaluate from its counterclockwise neighbors for ensuring the connectivity and success of Basil can be relaxed to  $S < b + 1$  while guaranteeing the success of*

---

### Algorithm 1: Basil

---

```

1 Input:  $\mathcal{N}$ (nodes);  $S$ (connectivity) ;  $\{\mathcal{Z}_i\}_{i \in \mathcal{N}}$ (local
  datasets);  $\mathbf{x}^0$ (initial model);  $K$ (number of rounds)
2 Initialization:
3 for each node  $i \in \mathcal{N}$  do
4   StoredModels [ $i$ ].insert( $\mathbf{x}^0$ ) // queue
   “StoredModels [ $i$ ]” is used by node  $i$  to keep the
   last inserted  $S$  models, denoted by  $\mathcal{N}^i$ . It is
   initialized by inserting  $\mathbf{x}^0$ 
5 end
6 Order  $\leftarrow$  RandomOrderAgreement( $\mathcal{N}$ ) // users’ order
  generation for the logical ring topology according to
  Section III-A.
7
8 Robust Training:
9 for each round  $k = 1, \dots, K$  do
10  for each node  $i = 1, \dots, N$  in sequence do
11    if node  $i \in$  benign set  $\mathcal{R}$  then
12       $\bar{\mathbf{x}}_k^{(i)} \leftarrow \mathcal{A}_{\text{Basil}}(\mathcal{N}^i)$  // Basil
      performance-based strategy to select one
      model from  $\mathcal{N}^i$  using (3)
13       $\mathbf{x}_k^{(i)} \leftarrow \text{Update}(\bar{\mathbf{x}}_k^{(i)}, \mathcal{Z}_i)$  // model update
      using (2)
14    end
15    else
16       $\mathbf{x}_k^{(i)} \leftarrow *$  // Byzantine node sends faulty
      model
17    end
18    multicast  $\mathbf{x}_k^{(i)}$  to the next  $S$  clockwise
    neighbors
19    for neighbor  $s = 1, \dots, S$  do
20      StoredModels [ $(i + s) \bmod N$ ].
      insert( $\mathbf{x}_k^{(i)}$ ) // insert  $\mathbf{x}_k^{(i)}$  to the queue of
      the  $s$ -th neighbor of node  $i$ 
21    end
22  end
23 end
24 Return  $\{\mathbf{x}_K^{(i)}\}_{i \in \mathcal{N}}$ 

```

---

Basil (benign subgraph connectivity) with high probability. Additionally, the failure probability of Basil is given by

$$\mathbb{P}(\text{Failure}) \leq \frac{b!(N - S)!}{(b - S)!(N - 1)!}, \quad (4)$$

where  $N$ ,  $b$  are the total number of nodes, and Byzantine nodes, respectively. The proofs of Proposition 1-2 are given in Appendix A.

*Remark 1:* In order to further illustrate the impact of choosing  $S$  on the probability of failure given in (4), we consider the following numerical examples. Let the total number of nodes in the system be  $N = 100$ , where  $b = 33$  of them are Byzantine, and the storage parameter  $S = 15$ . The failure event probability in (4) turns out to be  $\sim 4 \times 10^{-7}$ , which is negligible. For the case when  $S = 10$ , the probability of failure becomes  $\sim 5.34 \times 10^{-4}$ , which remains reasonably small.

## B. Theoretical Guarantees

We derive the convergence guarantees of `Basil` under the following standard assumptions.

**Assumption 1** (IID data distribution). *Local dataset  $\mathcal{Z}_i$  at node  $i$  consists of IID data samples from a distribution  $\mathcal{P}_i$ , where  $\mathcal{P}_i = \mathcal{P}$  for  $i \in \mathcal{R}$ . In other words,  $f_i(\mathbf{x}) = \mathbb{E}_{\zeta_i \sim \mathcal{P}_i}[l(\mathbf{x}, \zeta_i)] = \mathbb{E}_{\zeta_j \sim \mathcal{P}_j}[l(\mathbf{x}, \zeta_j)] = f_j(\mathbf{x}) \forall i, j \in \mathcal{R}$ . Hence, the global loss function  $f(\mathbf{x}) = \mathbb{E}_{\zeta_i \sim \mathcal{P}_i}[l(\mathbf{x}, \zeta_i)]$ .*

**Assumption 2** (Bounded variance). *Stochastic gradient  $g_i(\mathbf{x})$  is unbiased and variance bounded, i.e.,  $\mathbb{E}_{\mathcal{P}_i}[g_i(\mathbf{x})] = \nabla f_i(\mathbf{x}) = \nabla f(\mathbf{x})$ , and  $\mathbb{E}_{\mathcal{P}_i} \|g_i(\mathbf{x}) - \nabla f_i(\mathbf{x})\|^2 \leq \sigma^2$ , where  $g_i(\mathbf{x})$  is the stochastic gradient computed by node  $i$  by using a random sample  $\zeta_i$  from its local dataset  $\mathcal{Z}_i$ .*

**Assumption 3** (Smoothness). *The loss functions  $f_i^l$ s are  $L$ -smooth and twice differentiable, i.e., for any  $\mathbf{x} \in \mathbb{R}^d$ , we have  $\|\nabla^2 f_i(\mathbf{x})\|_2 \leq L$ .*

Let  $b^i$  be the number of counterclockwise Byzantine neighbors of node  $i$ . We divide the set of stored models  $\mathcal{N}_k^i$  at node  $i$  in the  $k$ -th round into two sets. The first set  $\mathcal{G}_k^i = \{\mathbf{y}_1, \dots, \mathbf{y}_{r^i}\}$  contains the benign models, where  $r^i = S - b^i$ . We consider scenarios with  $S = b + 1$ , where  $b$  is the total number of Byzantine nodes in the network. Without loss of generality, we assume the models in this set are arranged such that the first model is the closest benign node in the neighborhood of node  $i$ , while the last model is the farthest node. Similarly, we define the second set  $\mathcal{B}_k^i$  to be the set of models from the counterclockwise Byzantine neighbors of node  $i$  such that  $\mathcal{B}_k^i \cup \mathcal{G}_k^i = \mathcal{N}_k^i$ .

*Theorem 1:* When the learning rate  $\eta_k^{(i)}$  for node  $i \in \mathcal{R}$  in round  $k$  satisfies  $\eta_k^{(i)} \geq \frac{1}{L}$ , the expected loss function  $\mathbb{E}[l_i(\cdot)]$  of node  $i$  evaluated on the set of models in  $\mathcal{N}_k^i$  can be arranged as follows:

$$\mathbb{E}[l_i(\mathbf{y}_1)] \leq \mathbb{E}[l_i(\mathbf{y}_2)] \leq \dots \leq \mathbb{E}[l_i(\mathbf{y}_{r^i})] < \mathbb{E}[l_i(\mathbf{x})] \quad \forall \mathbf{x} \in \mathcal{B}_k^i, \quad (5)$$

where  $\mathcal{G}_k^i = \{\mathbf{y}_1, \dots, \mathbf{y}_{r^i}\}$  is the set of benign models stored at node  $i$ . Hence, the `Basil` aggregation rule in Definition 1 is reduced to  $\bar{\mathbf{x}}_k^{(i)} = \mathcal{A}_{\text{Basil}}(\mathcal{N}_k^i) = \mathbf{y}_1$ . Hence, the model update step in (2) can be simplified as follows:

$$\mathbf{x}_k^{(i)} = \mathbf{y}_1 - \eta_k^{(i)} g_i(\mathbf{y}_1). \quad (6)$$

*Remark 2:* For the `Basil` aggregation rule in Definition 1, (5) in Theorem 1 implies that for convergence analysis, we can consider only the benign sub-graph which is generated by removing the Byzantine nodes. As described in Section III-A, the benign sub-graph is connected. Furthermore, due to (6) in Theorem 1, training via `Basil` reduces to sequential training over a logical ring with only the set  $\mathcal{R}$  of benign nodes and connectivity parameter  $S = 1$ .

Leveraging the results in Theorem 1 and based on the discussion in Remark 1, we prove the linear convergence rate for `Basil`, under the additional assumption of convexity of the loss functions.

*Theorem 2:* Assume that  $f(\mathbf{x})$  is convex. Under Assumptions 1-3 stated in this section, `Basil` with a fixed learning

rate  $\eta = \frac{1}{L}$  at all users achieves linear convergence with a constant error as follows:

$$\mathbb{E} \left[ f \left( \frac{1}{T} \sum_{s=1}^T \mathbf{x}^s \right) \right] - f(\mathbf{x}^*) \leq \frac{\|\mathbf{x}^0 - \mathbf{x}^*\|^2 L}{2T} + \frac{1}{L} \sigma^2, \quad (7)$$

where  $T = Kr$ ,  $K$  is the total number of rounds over the ring and  $r$  is the number of benign nodes. Here  $\mathbf{x}^s$  represents the model after  $s$  update steps starting from the initial model  $\mathbf{x}^0$ , where  $s = rk + i$  with  $i = 1, \dots, r$  and  $k = 0, \dots, K - 1$ . Furthermore,  $\mathbf{x}^*$  is the optimal solution in (1) and  $\sigma^2$  is defined in Assumption 2.

*Remark 3:* The error bound for `Basil` decreases with increasing the total number of benign nodes  $r = \beta N$ , where  $\beta \in (0, 1)$ .

To extend `Basil` to be robust against software/hardware faults in the non-IID setting, i.e., when the local dataset  $\mathcal{Z}_i$  at node  $i$  consists of data samples from a distribution  $\mathcal{P}_i$  with  $\mathcal{P}_i \neq \mathcal{P}_j$  for  $i, j \in \mathcal{N}$  and  $i \neq j$ , we present our Anonymous Cyclic Data Sharing algorithm (ACDS) in the following section.

## IV. GENERALIZING BASIL TO NON-IID SETTING VIA ANONYMOUS CYCLIC DATA SHARING

We propose Anonymous Cyclic Data Sharing (ACDS), an algorithm that can be integrated on the top of `Basil` to guarantee robustness against software/hardware faults in the non-IID setting. This algorithm allows each node to anonymously share a fraction of its local *non-sensitive* dataset with other nodes. In other words, ACDS guarantees that the identity of the owner of the shared data is kept hidden from all other nodes under no collusion between nodes.

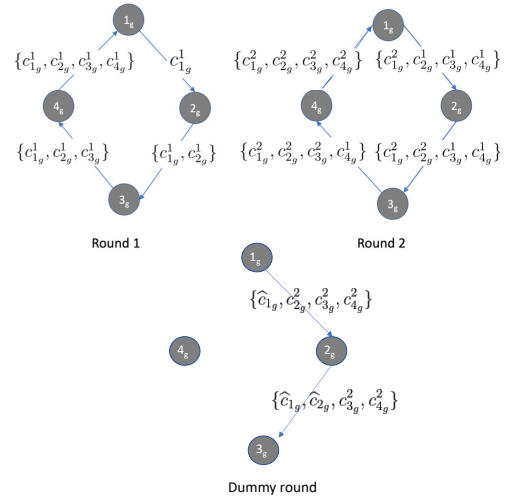


Fig. 3. ACDS algorithm within group  $g$  with  $n = 4$  users, where each node  $i_g \in \mathcal{N}_g$  has two batches  $\{c_{i_g}^1, c_{i_g}^2\}$ . Each round starts from node  $1_g$  and continues in a clockwise order. The dummy round is introduced to make sure that node  $2_g$  and node  $3_g$  get their missing batches  $\{c_{3_g}^2, c_{4_g}^2\}$  and  $c_{4_g}^2$ , respectively. Here,  $\hat{c}_{i_g}$  represents the dummy batch with the same size as the other batches that are used by node  $i_g \in \mathcal{N}_g$ . This dummy batch could be a batch of public data that shares the same features that are used in the learning task.

### A. ACDS Algorithm

The ACDS procedure has three phases which are formally described next. The overall algorithm has been summarized in Algorithm 2 and illustrated in Fig. 3.

**Phase 1: Initialization.** ACDS starts by first clustering the  $N$  nodes into  $G$  groups of rings, where the set of nodes in each group  $g \in [G]$  is denoted by  $\mathcal{N}_g = \{1_g, \dots, n_g\}$ . Here, node  $1_g$  is the starting node in ring  $g$ , and without loss of generality, we assume all groups have the same size  $n = \frac{N}{G}$ . Node  $i_g \in \mathcal{N}_g$  for  $g \in [G]$  divides its dataset  $\mathcal{Z}_{i_g}$  into sensitive ( $\mathcal{Z}_{i_g}^s$ ) and non-sensitive ( $\mathcal{Z}_{i_g}^{ns}$ ) portions, which can be done during the data processing phase by each node. Then, for a given hyperparameter  $\alpha \in (0, 1)$ , each node selects  $\alpha D$  points from its local non-sensitive dataset at random, where  $|\mathcal{Z}_{i_g}| = D$ , and then partitions these data points into  $H$  batches denoted by  $\{c_{i_g}^1, \dots, c_{i_g}^H\}$ , where each batch has  $M = \frac{\alpha D}{H}$  data points.

**Phase 2: Within Group Anonymous Data Sharing.** In this phase, for  $g \in [G]$ , the set of nodes  $\mathcal{N}_g$  in group  $g$  anonymously share their data batches  $\{c_{1_g}^j, \dots, c_{n_g}^j\}_{j \in [H]}$  with each other. The anonymous data sharing within group  $g$  takes  $H + 1$  rounds. In particular, as shown in Fig. 3, within group  $g$  and during the first round  $h = 1$ , node  $1_g$  sends the first batch  $c_{1_g}^1$  to its clockwise neighbor, node  $2_g$ . Node  $2_g$  then stores the received batch. After that, node  $2_g$  augments the received batch with its own first batch  $c_{2_g}^1$  and shuffles them together before sending them to node  $3_g$ . More generally, in the intra-group cyclic sharing over the ring, node  $i_g$  stores the received set of shuffled data points from batches  $\{c_{1_g}^1, \dots, c_{(i-1)_g}^1\}$  from its counterclockwise neighbor node  $(i-1)_g$ . Then, it adds its own batch  $c_{i_g}^1$  to the received set of data points, and shuffles them together, before sending the combined and shuffled dataset to node  $(i+1)_g$ .

For round  $1 < h \leq H$ , as shown in Fig. 3-(round 2), node  $1_g$  has the data points from the set of batches  $\{c_{1_g}^{(h-1)}, \dots, c_{n_g}^{(h-1)}\}$  which were received from node  $n_g$  at the end of round  $(h-1)$ . It first removes its old batch of data points  $c_{1_g}^{(h-1)}$  and then stores the remaining set of data points. After that, it adds its  $h$ -th batch,  $c_{1_g}^{(h)}$  to this remaining set, and then shuffles the entire set of data points in the new set of batches  $\{c_{1_g}^h, c_{2_g}^{h-1}, \dots, c_{n_g}^{h-1}\}$ , before sending them to node  $2_g$ . More generally, in the  $h$ -th round for  $1 < h \leq H$ , node  $i_g$  first removes its batch  $c_{i_g}^{h-1}$  from the received set of batches and then stores the set of remaining data points. Thereafter, node  $i_g$  adds its  $c_{i_g}^h$  to the set  $\{c_{1_g}^h, \dots, c_{(i-1)_g}^h, c_{(i)_g}^{h-1}, \dots, c_{n_g}^{h-1}\} \setminus \{c_{i_g}^{h-1}\}$ , and then shuffles the set of data points in the new set of batches  $\{c_{1_g}^h, \dots, c_{i_g}^h, c_{(i+1)_g}^{h-1}, \dots, c_{n_g}^{h-1}\}$  before sending them to node  $(i+1)_g$ .

After  $H$  intra-group communication iterations within each group as described above, all nodes within each group have completely shared their  $H - 1$  batches with each other. However, due to the sequential nature of unicast communications, some nodes are still missing the batches shared by some clients in the  $H^{\text{th}}$  round. For instance, in Fig. 3, after the completion of the second round, node  $2_g$  is missing the last batches  $c_{3_g}^2$  and  $c_{4_g}^2$ . Therefore, we propose a final *dummy* round, in which we repeat the same procedure adopted in rounds  $1 < h \leq H$ , but with the following slight modification: node  $i_g$  replaces

---

### Algorithm 2: ACDS

---

```

25 Input:  $\mathcal{N}$  (nodes);  $\{\mathcal{Z}_i\}_{i \in \mathcal{N}}$  (local datasets);  $\alpha$  (data
    fraction);  $H$  (number of batches);  $G$  (number of groups)
26 Phase 1: Initialization
27  $\{\mathcal{N}_g\}_{g \in [G]} \leftarrow$  Clustering ( $\mathcal{N}, G$ ) // cluster nodes  $\mathcal{N}$ 
    into  $G$  groups each of size  $n$ 
28 for each node  $i_g \in \mathcal{N}_g$  in parallel do
29    $\mathcal{Z}_{i_g}^s \cup \mathcal{Z}_{i_g}^{ns} \leftarrow$  Partition( $\mathcal{Z}_{i_g}$ ) // partition local data
     $\mathcal{Z}_{i_g}$  into sensitive and non-sensitive parts.
30    $\{c_{i_g}^1, \dots, c_{i_g}^H\} \leftarrow$  RandomSelection( $\mathcal{Z}_{i_g}^{ns}, \alpha, H$ ) //
    random selection of  $H$  batches, each of size  $\frac{\alpha D}{H}$ ,
    from  $\mathcal{Z}_{i_g}^{ns}$ .
31   DStored[ $i_g$ ] = list() // a list used by node  $i_g$  to
    store the shared data from other nodes
32 end
33 DShared[ $g$ ] = list(),  $\forall g \in [G]$  // a list that is used to
    circulate the data within group  $g$ 
34
35 Phase 2: Within Group Anonymous Data Sharing
36 for each group  $g = 1, \dots, G$  in parallel do
37   for each batch  $h = 1, \dots, H$  do
38     for each node  $i_g \in \mathcal{N}_g$  in sequence do
39       DShared[ $g$ ]; DStored[ $i_g$ ]  $\leftarrow$ 
         RobustShare(DShared[ $g$ ]; DStored[ $i_g$ ],
          $g, i_g, c_{i_g}^{h-1}, c_{i_g}^h$ )
40       Send DShared[ $g$ ] to the next clockwise
         neighbor
41     end
42   end
43   // start the dummy round
44   for each node  $i_g \in \mathcal{N}_g \setminus \{1_g, n_g\}$  in parallel do
45     DShared[ $g$ ]; DStored[ $i_g$ ]  $\leftarrow$ 
       RobustShare(DShared[ $g$ ]; DStored[ $i_g$ ],  $g$ ,
        $i_g, H, c_{i_g}^H, \widehat{c}_{i_g}$ )
46   end
47 end
48 Function RobustShare (DShared[ $g$ ]; DStored[ $i_g$ ],  $g$ ,
     $i_g, h, c_{i_g}^{h-1}, c_{i_g}^h$ ):
49   if  $h > 1$  then
50     DShared[ $g$ ].remove( $c_{i_g}^{h-1}$ ) // remove the batch
        $c_{i_g}^{h-1}$  from "DataShared[ $g$ ]"
51   end
52   DStored[ $i_g$ ].add(DShared[ $g$ ]) // copy the data in
       "DShared[ $g$ ]" to "DStored[ $i_g$ ]"
53   DShared[ $g$ ].add( $c_{i_g}^h$ ) // add the  $h$ -th batch  $c_{i_g}^h$  that
       will be shared with other nodes to "DShared[ $g$ ]"
54   DShared[ $g$ ].shuffle() //shuffle the data in the list
       "DShared[ $g$ ]"
55   return DShared[ $g$ ]; DStored[ $i_g$ ]
56
57 Phase 3: Global Sharing
58 for  $g = 1, \dots, G$  in parallel do
59   node  $1_g$  multicasts DStored[ $1_g$ ]  $\cup \{c_{1_g}^1, \dots, c_{1_g}^H\}$ 
       with all nodes in  $\bigcup_{g' \in [N] \setminus \{g\}} \mathcal{N}_{g'}$ 
60 end
61

```

---

its batch  $c_{i_g}^H$  with a dummy batch  $c_{i_g}^{\text{dummy}}$ . This dummy batch could be a batch of public data points that share the same feature space that is used in the learning task. This completes the anonymous cyclic data sharing within group  $g \in [G]$ .

**Phase 3: Global Sharing.** For each  $g \in [G]$ , node  $1_g$  shares the dataset  $\{c_{1_g}^1, \dots, c_{n_g}^j\}_{j \in [H]}$ , which it has gathered in phase 2, with all other nodes in the other groups.

We note that implementation of ACDS only needs to be done once before training. As we demonstrate later in Section VI, the one-time overhead of the ACDS algorithm dramatically improves convergence performance when data is non-IID. In the following proposition, we describe the communication cost/time of ACDS.

**Proposition 3** (Communication cost/time of ACDS). *Consider ACDS algorithm with a set of  $N$  nodes divided equally into  $G$  groups with  $n$  nodes in each group. Each node  $i \in [N]$  has  $H$  batches each of size  $M = \frac{\alpha D}{H}$  data points, where  $\alpha D$  is the fraction of shared local data, such that  $\alpha \in (0, 1)$  and  $D$  is the local data size. By letting  $I$  to be the size of each data point in bits, we have the following:*

(1) Worst case communication cost per node ( $C_{ACDS}$ )

$$C_{ACDS} = \alpha DI \left( \frac{1}{H} + n(G+1) \right). \quad (8)$$

(2) Total communication time for completing ACDS ( $T_{ACDS}$ )

When the upload/download bandwidth of each node is  $R$  b/s, we have the following

$$T_{ACDS} = \frac{\alpha DI}{HR} [n^2(H+0.5) + n(H(G-1) - 1.5)]. \quad (9)$$

*Remark 4:* The worst case communication cost in (8) is with respect to the first node  $1_g$ , for  $g \in [G]$ , that has more communication cost than the other nodes in group  $g$  for its participation in the global sharing phase of ACDS.

*Remark 5:* To illustrate the communication overhead resulting from using ACDS, we consider the following numerical example. Let the total number of nodes in the system be  $N = 100$  and each node has  $D = 500$  images from the CIFAR10 dataset, where each image of size  $I = 24.5$  Kbits<sup>1</sup>. When the communication bandwidth at each node is  $R = 100$  Mb/s (e.g., 4G speed), and each node shares only  $\alpha = 5\%$  of its dataset in the form of  $H = 5$  batches each with size  $M = 5$  images, the latency, and communication cost of ACDS with  $G = 4$  groups are 11 seconds and 75 Mbits, respectively. We note that the communication cost for ACDS and completion time of the algorithm are small with respect to the training process that requires sharing large model for large number of iteration as demonstrated in Section VI.

The proof of Proposition 3 is presented in Appendix D.

In the following, we discuss the anonymity guarantees of ACDS.

### B. Anonymity Guarantees of ACDS

In the first round of the scheme, node  $2_g$  will know that the source of the received batch  $c_{1_g}^1$  is node  $1_g$ . Similarly and

more general, node  $i_g$  will know that each data point in the received set of batches  $\{c_{1_g}^1, \dots, c_{(i-1)_g}^1\}$  is generated by one of the previous  $i-1$  counterclockwise neighbors. However, in the next  $H-1$  rounds, each received data point by any node will be equally likely generated from any one of the remaining  $n-1$  nodes in this group. Hence, the size of the candidate pool from which each node could take a guess for the owner of each data point is small specially for the first set of nodes in the ring. In order to provide anonymity for the entire data and decrease the risk in the first round of the ACDS scheme, the size of the batch can be reduced to just one data point. Therefore, in the first round node  $2_g$  will only know one data point from node  $1_g$ . This comes on the expense of increasing the number of rounds. Another key consideration is that the number of nodes in each group trades the level of anonymity with the communication cost. In particular, the communication cost per node in the ACDS algorithm is  $\mathcal{O}(n)$ , while the anonymity level, which we measure by the number of possible candidates for a given data point, is  $(n-1)$ . Therefore, increasing  $n$ , i.e., decreasing the number of groups  $G$ , will decrease the communication cost but increase the anonymity level.

## V. BASIL+: PARALLELIZATION OF BASIL

In this section, we describe our modified protocol `Basil+` which allows for parallel training across multiple rings, along with sequential training over each ring. This results in decreasing the training time needed for completing one global epoch (visiting all nodes) compared to `Basil` which only considers sequential training over one ring.

### A. Basil+ Algorithm

At a high level, `Basil+` divides nodes into  $G$  groups such that each group in parallel performs sequential training over a logical ring using `Basil` algorithm. After  $\tau$  rounds of sequential training within each group, a robust circular aggregation strategy is implemented to have a robust average model from all the groups. Following the robust circular aggregation stage, a final multicasting step is implemented such that each group can use the resulting robust average model. This entire process is repeated for  $K$  global rounds.

We now formalize the execution of `Basil+` through the following four stages.

**Stage 1: Basil+ Initialization.** The protocol starts by clustering the set of  $N$  nodes equally into  $G$  groups of rings with  $n = \frac{N}{G}$  nodes in each group. The set of nodes in group  $g$  is denoted by  $\mathcal{N}_g = \{u_1^g, \dots, u_n^g\}$ , where node  $u_1^g$  is the starting node in ring  $g$ , where  $g = 1, \dots, G$ . The clustering of nodes follows a random splitting agreement protocol similar to the one in Section III-A (details are presented in Section V-B). The connectivity parameter within each group is set to be  $S = \min(n-1, b+1)$ , where  $b$  is the worst-case number of Byzantine nodes. This choice of  $S$  guarantees that each benign subgraph within each group is connected with high probability, as described in Proposition 3.

<sup>1</sup>Each image in CIFAR10 dataset has 3 channels each of size  $32 \times 32$  pixels, and each pixel takes value from 0 – 255.



**Stage 2: Within Group Parallel Implementation of Basil.**

Each group  $g \in [G]$  in parallel performs the training across its nodes for  $\tau$  rounds using Basil algorithm.

**Stage 3: Robust Circular Aggregation Strategy.** We denote

$$\mathcal{S}_g = \{u_{n-1}^g, u_{n-2}^g, \dots, u_{n-S+1}^g\}, \quad (10)$$

to be the set of  $S$  counterclockwise neighbors of node  $u_1^g$ . The robust circular aggregation strategy consists of  $G-1$  steps performed sequentially over the  $G$  groups, where the  $G$  groups form a global ring. At step  $g$ , where  $g \in \{1, \dots, G-1\}$ , the set of nodes  $\mathcal{S}_g$  send their aggregated models to each node in the set  $\mathcal{S}_{g+1}$ . The reason for sending  $S$  models from one group to another is to ensure the connectivity of the global ring when removing the Byzantine nodes. The average aggregated model at node  $u_i^{g+1} \in \mathcal{S}_{g+1}$  is given as follows:

$$\mathbf{z}_i^{g+1} = \frac{1}{g+1} \left( \mathbf{x}_\tau^{(i,g+1)} + g\bar{\mathbf{z}}_i^{g+1} \right), \quad (11)$$

where  $\mathbf{x}_\tau^{(i,g+1)}$  is the local updated model at node  $u_i^{g+1}$  in ring  $g+1$  after  $\tau$  rounds of updates according to Basil algorithm. Here,  $\bar{\mathbf{z}}_i^{g+1}$  is the selected model by node  $u_i^{g+1}$  from the set of received models from the set  $\mathcal{S}_g$ . More specifically, by letting

$$\mathcal{L}_g = \{\mathbf{z}_{n-1}^g, \mathbf{z}_{n-2}^g, \dots, \mathbf{z}_{n-S+1}^g\} \quad (12)$$

be the set of average aggregated models sent from the set of nodes  $\mathcal{S}_g$  to each node in the set  $\mathcal{S}_{g+1}$ , we define  $\bar{\mathbf{z}}_i^{g+1}$  to be the model selected from  $\mathcal{L}_g$  by node  $u_i^{g+1} \in \mathcal{S}_{g+1}$  using the Basil aggregation rule as follows:

$$\bar{\mathbf{z}}_i^{g+1} = \mathcal{A}_{\text{Basil}}(\mathcal{L}_g) = \arg \min_{\mathbf{y} \in \mathcal{L}_g} \mathbb{E} \left[ l_i^{g+1}(\mathbf{y}, \zeta_i^{g+1}) \right]. \quad (13)$$

**Stage 4: Robust Multicasting.** The final stage is the multicasting stage. The set of nodes in  $\mathcal{S}_G$  send the final set of robust aggregated models  $\mathcal{L}_G$  to  $\mathcal{S}_1$ . Each node in the set  $\mathcal{S}_1$  applies the aggregation rule in (13) on the set of received models  $\mathcal{L}_G$ . Finally, each benign node in the set  $\mathcal{S}_1$  sends the filtered model  $\mathbf{z}_i^1$  to all nodes in this set  $\cup_{g=1}^G \mathcal{U}_g$ , where  $\mathcal{U}_g$  is defined as follows

$$\mathcal{U}_g = \{u_1^g, u_2^g, \dots, u_S^g\}. \quad (14)$$

Finally, all nodes in this set  $\cup_{g=1}^G \mathcal{U}_g$  use the aggregation rule in (13) to get the best model out of this set  $\mathcal{L}_1$  before updating it according to (2). These four stages are repeated for  $K$  rounds.

We compare between the training time of Basil and Basil+ in the following proposition.

**Proposition 4.** Let  $T_{\text{comm}}$ ,  $T_{\text{perf-based}}$ , and  $T_{\text{SGD}}$  respectively denote the time needed to multicast/receive one model, the time to evaluate  $S$  models according to Basil performance-based criterion, and the time to take one step of model update. The total training time for completing one global round when using Basil algorithm, where one global round consists of  $\tau$  sequential rounds over the ring, is

$$T_{\text{Basil}} \leq (\tau n G) T_{\text{perf-based}} + (\tau n G) T_{\text{comm}} + (\tau n G) T_{\text{SGD}}, \quad (15)$$

**Algorithm 3: Basil+**


---

```

62 Input:  $\mathcal{N}; S; \{\mathcal{Z}_i\}_{i \in \mathcal{N}}; \mathbf{x}^0; \tau, K$ 
63 Stage 1: Initialization:
64 for each node  $i \in \mathcal{N}$  do
65    $\{\mathcal{N}_g\}_{g \in [G]} \leftarrow \text{RandomClusteringAgreement}(\mathcal{N}, G)$ 
   //cluster the nodes into  $G$  groups each of size  $n$ 
   according to Section IV-A
66 end
67  $\mathbf{x}^{(i,g)} \leftarrow \mathbf{x}^0, \quad \forall i \in \mathcal{N}_g, g \in [G]$ 
68 for each global round  $k = 1, \dots, K$  do
69   Stage 2: Within Groups Robust Training:
70   for each group  $g = 1, \dots, G$  in parallel do
71      $\text{Basil}(\mathcal{N}_g, S, \{\mathcal{Z}_i\}_{i \in \mathcal{N}_g}, \{\mathbf{x}^{(i,g)}\}_{i \in \mathcal{N}_g}, \tau) \rightarrow$ 
      $\{\mathbf{x}_\tau^{(i,g)}\}_{i \in \mathcal{N}_g}$  //apply Basil algorithm within
     each group for  $\tau$  rounds
72      $\mathbf{z}_i^g \leftarrow \mathbf{x}_\tau^{(i,g)}, \quad \forall i \in \mathcal{N}_g$ 
73   end
74
75   Stage 3: Robust Circular Aggregation: for each
   group  $g = 1, \dots, G-1$  in sequence do
76     for each node  $u_i^{g+1} \in \mathcal{S}_{g+1}$  in parallel do
77       // the set  $\mathcal{S}_{g+1}$  is defined in (10)
78        $\mathcal{L}_g \leftarrow \{\mathbf{z}_i^g\}_{u_i^g \in \mathcal{S}_g}$  // each node
        $u_i^{g+1} \in \mathcal{S}_{g+1}$  receives the set of models
        $\mathcal{L}_g$  (defined in (12)) from the nodes in  $\mathcal{S}_g$ .
79       if node  $u_i^{g+1} \in$  benign set  $\mathcal{R}$  then
80          $\bar{\mathbf{z}}_i^{g+1} \leftarrow \mathcal{A}_{\text{Basil}}(\mathcal{L}_g)$  // Basil
         performance based strategy to select
         one model from  $\mathcal{L}_g$  using (13)
81          $\mathbf{z}_i^{g+1} \leftarrow \frac{1}{g+1} \left( \mathbf{x}_\tau^{(i,g+1)} + g\bar{\mathbf{z}}_i^{g+1} \right)$  //get
         proper average model from the first
          $g+1$  groups
82       end
83       else
84          $\mathbf{z}_i^{g+1} \leftarrow *$  // Byzantine node sends
         faulty model
85       end
86     end
87   end
88
89   Stage 4: Robust Multicasting:
90   for each node  $u_i^1 \in \mathcal{S}_1$  in parallel do
91      $\mathcal{L}_G \leftarrow \{\mathbf{z}_i^{(G)}\}_{u_i^G \in \mathcal{S}_G}$ .
92      $\bar{\mathbf{z}}_i^1 \leftarrow \mathcal{A}_{\text{Basil}}(\mathcal{L}_G)$ 
93      $\mathbf{z}_i^1 \leftarrow \bar{\mathbf{z}}_i^1$ 
94   end
95   for each node  $u_i^g \in \cup_{g=1}^G \mathcal{U}_g$  in parallel do
96     // the set  $\mathcal{U}_g$  is defined in (14)  $\mathcal{L}_1 \leftarrow \{\mathbf{z}_i^1\}_{u_i^1 \in \mathcal{S}_1}$ 
     // each node  $u_i^g$  receives the set of models  $\mathcal{L}_1$ 
     from the nodes in  $\mathcal{S}_1$ .
97      $\bar{\mathbf{z}}_i^g \leftarrow \mathcal{A}_{\text{Basil}}(\mathcal{L}_1)$ 
98      $\mathbf{x}^{(i,g)} \leftarrow \bar{\mathbf{z}}_i^g$ 
99   end
100
101 end
102 Return  $\{\mathbf{x}_K^{(i,g)}\}_{i \in \mathcal{N}_g, g \in [G]}$ 

```

---

compared to the training time for *Basil+* algorithm, which is given as follows

$$T_{\text{Basil}+} \leq (\tau n + G + 1)T_{\text{perf-based}} + (SG + \tau n - 1)T_{\text{comm}} + (\tau n)T_{\text{SGD}}. \quad (16)$$

*Remark 6:* According to this proposition, we can see the training time of *Basil* is polynomial in  $nG$ , while in *Basil+*, the training time is linear in both  $n$  and  $G$ . The proof of Proposition 4 is given in Appendix E.

In the following section, we discuss the random clustering method used in the Stage 1 of *Basil+*.

## B. Random Clustering Agreement

In practice, nodes can agree on a random clustering by using similar approach as in Section III-A by the following simple steps. 1) All nodes first share their IDs with each other, and we assume WLOG that nodes' IDs can be arranged in ascending order, and Byzantine nodes cannot forge their identities or create multiple fake ones [27]. 2) Each node locally random splits the nodes into  $G$  subsets by using a pseudo random number generator (PRNG) initialized via a common seed (e.g.,  $N$ ). This ensures that all nodes will generate the set of nodes. To know the nodes order within each local group, the method in Section III-A can be used.

## C. The Success of *Basil+*

We will consider different scenarios for the connectivity parameter  $S$  while evaluating the success of *Basil+*. **Case 1:**  $S = \min(n - 1, b + 1)$  We set the connectivity parameter for *Basil+* to  $S = \min(n - 1, b + 1)$ . By setting  $S = b + 1$  when  $n > b + 1$ , this ensures the connectivity of each ring (after removing the Byzantine nodes) along with the global ring. On the other hand, by setting  $S = n - 1$  if  $n \leq b + 1$ , *Basil+* would only fail if at least one group has a number of Byzantine nodes of  $n$  or  $n - 1$ . We define  $B_j$  to be the failure event in which the number of Byzantine nodes in a given group is  $n$  or  $n - 1$ . The failure event  $B_j$  follows a Hypergeometric distribution with parameters  $(N, b, n)$ , where  $N$ ,  $b$ , and  $n$  are the total number of nodes, total number of Byzantine nodes, number of nodes in each group, respectively. The probability of failure is given as follows

$$\mathbb{P}(\text{Failure}) = \mathbb{P}\left(\bigcup_{j=1}^G B_j\right) \stackrel{(a)}{\leq} \sum_{j=1}^G \mathbb{P}(B_j) = \frac{\binom{b}{n} + \binom{b}{n-1} \binom{N-b}{1}}{\binom{N}{n}} G, \quad (17)$$

where (a) follows from the union bound.

In order to further illustrate the impact of choosing the group size  $n$  when setting  $S = n - 1$  on the probability of failure given in (17), we consider the following numerical examples. Let the total number of nodes in the system be  $N = 100$ , where  $b = 33$  of them are Byzantine. By setting  $n = 20$  nodes in each group, the probability in (17) turns out to be  $\sim 5 \times 10^{-10}$ , which is negligible. For the case when  $n = 10$ , the probability of failure becomes  $\sim 1.2 \times 10^{-4}$ , which remains reasonably small.

**Case 2:**  $S < n - 1$  Similar to the failure analysis of *Basil* given in Proposition 2, we relax the connectivity parameter  $S$  as stated in the following proposition.

**Proposition 5.** *The connectivity parameter  $S$  in *Basil+* can be relaxed to  $S < n - 1$  while guaranteeing the success of the algorithm (benign local/global subgraph connectivity) with high probability. The failure probability of *Basil+* is given by*

$$\mathbb{P}(F) \leq G \sum_{i=0}^{\min(b,n)} \left( \prod_{s=0}^{S-1} \frac{\max(i-s, 0)}{(N-s)} n \right) \frac{\binom{b}{i} \binom{N-b}{n-i}}{\binom{N}{n}}, \quad (18)$$

where  $N$ ,  $n$ ,  $G$ ,  $S$  and  $b$  are the number of total nodes, number of nodes in each group, number of groups, the connectivity parameter, and the number of Byzantine nodes.

The proof of Proposition 5 is presented in Appendix F.

*Remark 7:* In order to further illustrate the impact of choosing  $S$  on the probability of failure given in (18), we consider the following numerical examples. Let the total number of nodes in the system be  $N = 400$ , where  $b = 60$  of them are Byzantine and  $n = 100$ , and the connectivity parameter  $S = 10$ . The probability of failure event in (18) turns out to be  $\sim 10^{-6}$ , which is negligible. For the case when  $S = 7$ , the probability of failure becomes  $\sim 10^{-4}$ , which remains reasonably small.

## VI. NUMERICAL EXPERIMENTS

We start by evaluating the performance gains of *Basil*. After that, we give the set of experiments of *Basil+*. We note that in Appendix H, we have included additional experiments for *Basil* including the wall-clock time performance compared to UBAR, performance of *Basil* and ACDS for CIFAR100 dataset, and performance comparison between *Basil* and *Basil+*.

### A. Numerical Experiments for *Basil*

**Schemes:** We consider four schemes as described next.

- **G-plain:** This is for graph based topology. At the start of each round, nodes exchange their models with their neighbors. Each node then finds the average of its model with the received neighboring models and uses it to carry out an SGD step over its local dataset.
- **R-plain:** This is for ring based topology with  $S = 1$ . The current active node carries out an SGD step over its local dataset by using the model received from its previous counterclockwise neighbor.
- **UBAR:** This is the prior state-of-the-art for mitigating Byzantine nodes in decentralized training over graph, and is described in Appendix G.
- **Basil:** This is our proposal.

**Datasets and Hyperparameters:** There are a total of 100 nodes, in which 67 are benign. For decentralized network setting for simulating UBAR and G-plain schemes, we follow a similar approach as described in the experiments in [10] (we provide the details in Appendix H-B). For *Basil* and R-plain, the nodes are arranged in a logical ring, and 33 of them are randomly set as Byzantine nodes. Furthermore,

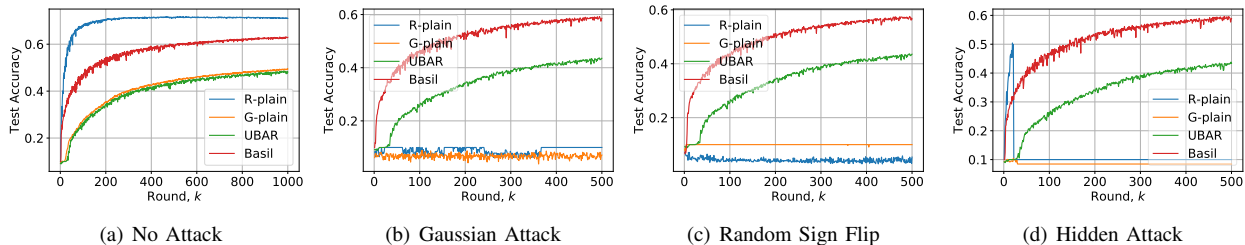


Fig. 4. Illustrating the performance of `Basil` using CIFAR10 dataset under IID data distribution setting.

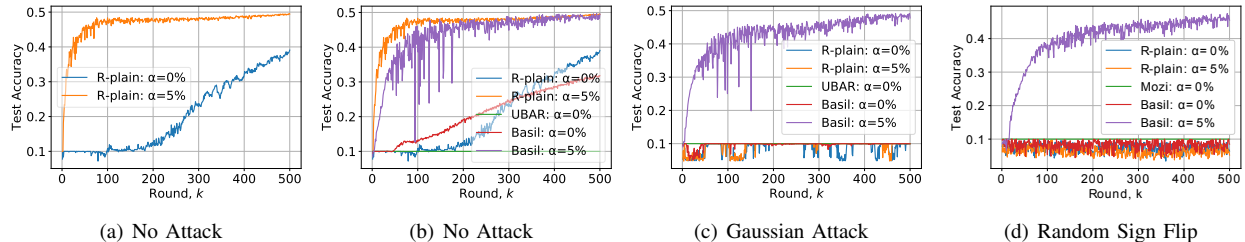


Fig. 5. Illustrating the performance of `Basil` using CIFAR10 dataset under non-IID data distribution setting.

we set  $S = 10$  for `Basil` which gives us the connectivity guarantees discussed in Proposition 2. We use a decreasing learning rate of  $0.03/(1+0.03k)$ . We consider CIFAR10 [28] and use a neural network with 2 convolutional layers and 3 fully connected layers. The details are included in Appendix H-A. The training dataset is partitioned equally among all nodes. Furthermore, we report the worst test accuracy among the benign clients in our results. We also conduct similar evaluations on the MNIST dataset. The experimental results lead to the same conclusion and can be found in Appendix H. Additionally, we emphasize that `Basil` is based on sequential training over a logical ring, while `UBAR` is based on parallel training over a graph topology. Hence, for consistency of experimental evaluations, we consider the following common definition for training round:

*Definition 2 (Training round):* With respect to the total number of SGD computations, we define a round over a logical ring to be equivalent to one parallel iteration over a graph. This definition aligns with our motivation of training with resource constrained edge devices, where user’s computation power is limited.

**Byzantine Attacks:** We consider a variety of attacks, that are described as follows. *Gaussian Attack:* Each Byzantine node replaces its model parameters with entries drawn from a Gaussian distribution with mean 0 and standard distribution  $\sigma = 1$ . *Random Sign Flip:* We observed in our experiments that the naive sign flip attack, in which Byzantine nodes flip the sign of each parameter before exchanging their models with their neighbors, is not strong in the R-plain scheme. To make the sign-flip attack stronger, we propose a layer-wise sign flip, in which Byzantine nodes randomly choose to flip or keep the sign of the entire elements in each neural network layer. *Hidden Attack:* This is the attack that degrades the performance of distance-based defense approaches, as proposed in [23]. Essentially, the Byzantine nodes are assumed

to be omniscient, i.e., they can collect the models uploaded by all the benign clients. Byzantine nodes then design their models such that they are undetectable from the benign ones in terms of the distance metric, while still degrading the training process. For hidden attack, as the key idea is to exploit similarity of models from benign nodes, thus, to make it more effective, the Byzantine nodes launch this attack after 20 rounds of training.

**Results (IID Setting):** We first present the results for the IID data setting. The training dataset is first shuffled randomly and then partitioned among the nodes. As can be seen from Fig. 4(a), `Basil` converges much faster than both `UBAR` and `G-plain` even in the absence of any Byzantine attacks, illustrating the benefits of ring topology based learning over graph based topology. We note that the total number of gradient updates after  $k$  rounds in the two setups are almost the same. We can also see that R-plain gives higher performance than `Basil`. This is because in `Basil`, a small mini-batch is used for performance evaluation, hence in contrast to R-plain, the latest neighborhood model may not be chosen in each round resulting in the loss of some update steps. Nevertheless, Figs. 4(b), (c) and 4(d) illustrate that `Basil` is not only Byzantine-resilient, it maintains its superior performance over `UBAR` with  $\sim 16\%$  improvement in test accuracy, as opposed to R-plain that suffers significantly. Furthermore, we would like to highlight that as `Basil` uses a performance-based criterion for mitigating Byzantine nodes, it is robust to the Hidden attack as well. Finally, by considering the poor convergence of R-plain under different Byzantine attacks, we conclude that `Basil` is a good solution with fast convergence, strong Byzantine resiliency and acceptable computation overhead.

**Results (non-IID Setting):** For simulating the non-IID setting, we sort the training data as per class, partition the sorted data into  $N$  subsets, and assign each node 1 partition. By applying ACDS in the absence of Byzantine nodes while trying different

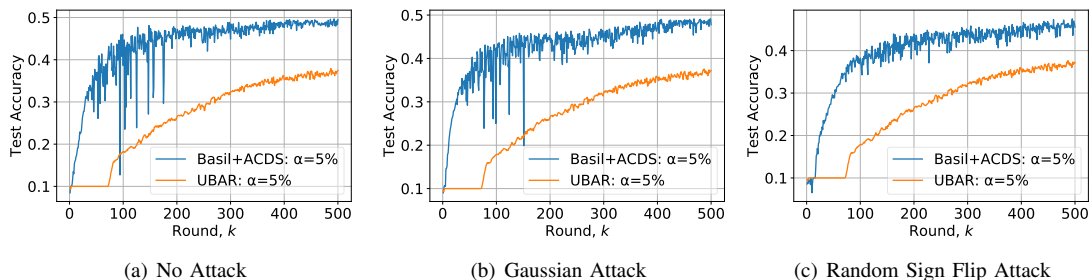


Fig. 6. Illustrating the performance of Basil compared with UBAR for CIFAR10 under non-IID data distribution setting with  $\alpha = 5\%$  data sharing.

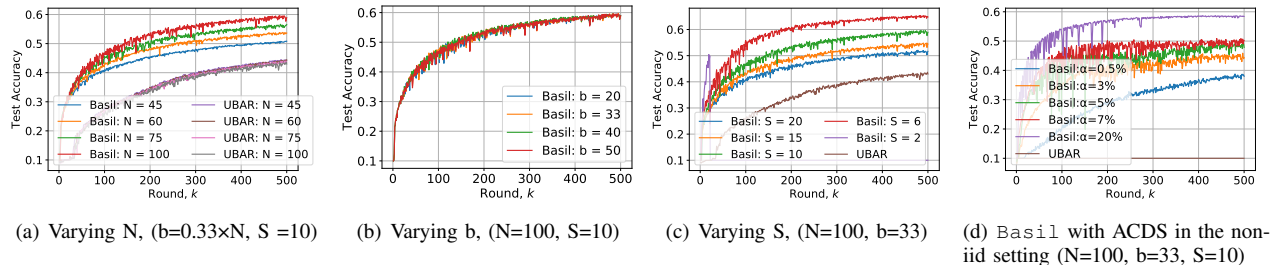


Fig. 7. Ablation studies. Here  $N$ ,  $b$ ,  $S$ ,  $\alpha$  are the total nodes, Byzantine nodes, connectivity, and fraction of shared data. For non-IID data, Gaussian attack is considered, while for others plots with IID hidden attack is used. Using the same NNs in Section H-A.

values for  $\alpha$ , we found that  $\alpha = 5\%$  gives a good performance while a small amount of shared data from each node. Fig. 5(a) illustrates that test accuracy for R-plain in the non-IID setting can be increased by up to  $\sim 10\%$  when each node shares only  $\alpha = 5\%$  of its local data with other nodes. Fig. 5(c), and Fig. 5(d) illustrate that Basil on the top of ACDS with  $\alpha = 5\%$  is robust to software/hardware faults represented in Gaussian model and random sign flip. Furthermore, both Basil without ACDS and UBAR completely fail in the presence of these faults. This is because the two defenses are using performance-based criterion which is not meaningful in the non-IID setting. In other words, each node has only data from one class, hence it becomes unclear whether a high loss value for a given model can be attributed to the Byzantine nodes, or to the very heterogeneous nature of the data. Additionally, R-plain with  $\alpha = 0\%, 5\%$  completely fail in the presence of these faults.

Furthermore, we can observe in Fig. 5(b) that Basil with  $\alpha = 0$  gives low performance. This confirms that non-IID data distribution degraded the convergence behavior. For UBAR, the performance is completely degraded, since in UBAR each node selects the set of models which gives a lower loss than its own local model, before using them in the update rule. Since performance-based is not meaningful in this setting, each node might end up only with its own model. Hence, the model of each node does not completely propagate over the graph, as also demonstrated in Fig. 5(b), where UBAR fails completely. This is different from the ring setting, where the model is propagated over the ring.

In Fig. 5, we showed that UBAR performs quite poorly for non-IID data setting, when no data is shared among the clients. We note that achieving anonymity in data sharing in graph based decentralized learning in general and UBAR in particular is an open problem. Nevertheless, in Fig. 6, we further

show that even 5% data sharing is done in UBAR, performance remains quite low in comparison to Basil+ACDS.

Now, we compute the communication cost overhead due to leveraging ACDS for the experiments associated with Fig. 5. By considering the setting discussed in Remark 5 for ACDS with  $G = 4$  groups for data sharing and each node sharing  $\alpha = 5\%$  fraction of its local dataset, we can see from Fig. 5 that Basil takes 500 rounds to get  $\sim 50\%$  test accuracy. Hence, given that the model used in this section is of size 3.6 Mbits (117706 trainable parameters each represented by 32 bits), the communication cost overhead resulting from using ACDS for data sharing is only 4%.

**Further ablation studies:** We perform ablation studies to show the effect of different parameters on the performance of Basil: number of nodes  $N$ , number of Byzantine nodes  $b$ , connectivity parameter  $S$ , and the fraction of data sharing  $\alpha$ . For the ablation studies corresponding to  $N$ ,  $b$ ,  $S$ , we consider the IID setting described previously, while for the  $\alpha$ , we consider the non-IID setting.

Fig. 7(a) demonstrates that, unlike UBAR, Basil performance scales with the number of nodes  $N$ . This is because in any given round, the sequential training over the logical ring topology accumulates SGD updates of clients along the logical ring, as opposed to parallel training over the graph topology in which an update from any given node only propagates to its neighbors. Hence, Basil has better accuracy than UBAR. Additionally, as described in Section V, one can also leverage Basil+ to achieve further scalability for large  $N$  by parallelizing Basil. We provide the experimental evaluations corresponding to Basil+ in Section VI-B.

To study the effect of different number of Byzantine nodes in the system, we conduct experiments with different  $b$ . Fig. 7(b) demonstrates that Basil is quite robust to different

number of Byzantine nodes.

Fig. 7(c) demonstrates the impact of the connectivity parameter  $S$ . Interestingly, the convergence rate decreases as  $S$  increases. We posit that due to the noisy SGD based training process, the closest benign model is not always selected, resulting in loss of some intermediate update steps. However, decreasing  $S$  too much results in larger increase in the connectivity failure probability of `Basil`. For example, the upper bound on the failure probability when  $S = 6$  is less than 0.09. However, for an extremely low value of  $S = 2$ , we observed consistent failure across all simulation trials, as also illustrated in Fig. 7(c). Hence, a careful choice of  $S$  is important.

Finally, to study the relationship between privacy and accuracy when `Basil` is used alongside ACDS, we carry out numerical analysis by varying  $\alpha$  in the non-IID setting described previously. Fig. 7(d) demonstrates that as  $\alpha$  is increased, i.e., as the amount of shared data is increased, the convergence rate increases as well. Furthermore, we emphasize that even having  $\alpha = 0.5\%$  gives reasonable performance when data is non-IID, unlike `UBAR` which fails completely.

### B. Numerical Experiments for `Basil+`

In this section, we demonstrate the achievable gains of `Basil+` in terms of its scalability, Byzantine robustness, and superior performance over `UBAR`.

**Schemes:** We consider three schemes, as described next.

- *Basil+*: Our proposed scheme.
- *R-plain+*: We implement a parallel extension of `R-plain`. In particular, nodes are divided into  $G$  groups. Within each group, a sequential `R-plain` training process is carried out, wherein the current active node carries out local training using the model received from its previous counterclockwise neighbor. After  $\tau$  rounds of sequential `R-plain` training within each group, a circular aggregation is carried out along the  $G$  groups. Specifically, the model from the last node in each group gets averaged. The average model from each group is then used by the first node in each group in the next global round. This entire process is repeated for  $K$  global rounds.

**Setting:** We use CIFAR10 dataset [28] and use the neural network with 2 convolutional layers and 3 fully connected layers described in Section VI. The training dataset is partitioned uniformly among the set  $\mathcal{N}$  of all nodes, where  $|\mathcal{N}| = 400$ . We set the batch size to 80 for local training and performance evaluation in `Basil+` as well as `UBAR`. Furthermore, we consider epoch based local training, where we set the number of epochs to 3. We use a decreasing learning rate of  $0.03/(1 + 0.03k)$ , where  $k$  denotes the global round. For all schemes, we report the average test accuracy among the benign clients. For `Basil+`, we set the connectivity parameter to  $S = 6$  and the number of intra-group rounds to  $\tau = 1$ . The implementation of `UBAR` is given in Section H-B.

**Results:** For studying how the three schemes perform when more nodes participate in the training process, we consider different cases for the number of participating nodes  $\mathcal{N}_a \subseteq \mathcal{N}$ , where  $|\mathcal{N}_a| = N_a$ . Furthermore, for the three schemes, we

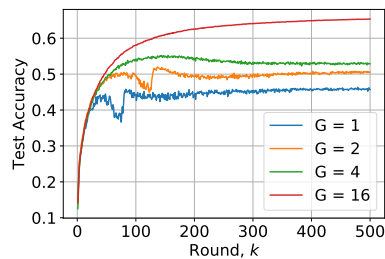


Fig. 8. The scalability gain of `Basil+` in the presence of Byzantine nodes as number of nodes increases. Here  $G$  is the number of groups, where each group has  $n = 25$  nodes.

set the total number of Byzantine nodes to be  $\lfloor \beta N_a \rfloor$  with  $\beta = 0.2$ .

Fig. 8 shows the performance of `Basil+` in the presence of Gaussian attack when the number of groups increases, i.e., when the number of participating nodes  $N_a$  increases. Here, for all the four scenarios in Fig. 8, we fix the number of nodes in each group to  $n = 25$  nodes. As we can see `Basil+` is able to mitigate the Byzantine behavior while achieving scalable performance as the number of nodes increases. In particular, `Basil+` with  $G = 16$  groups (i.e.,  $N_a = 400$  nodes) achieves a test accuracy which is higher by an absolute margin of 20% compared to the case of  $G = 1$  (i.e.,  $N_a = 25$  nodes). Additionally, while `Basil+` provides scalable model performance when the number of groups increases, the overall increase in training time scales gracefully due to parallelization of training within groups. In particular, the key difference in the training time between the two cases of  $G = 1$  and  $G = 16$  is in the stages of robust aggregation and global multicast. In order to get further insight, we set  $T_{\text{comm}}$ ,  $T_{\text{perf-based}}$  and  $T_{\text{SGD}}$  in equation (29) to one unit of time. Hence, using (29), one can show that the ratio of the training time for  $G = 16$  with  $N_a = 400$  nodes to the training time for  $G = 1$  with  $N_a = 25$  nodes is just 1.5. This further demonstrates the scalability of `Basil+`.

In Fig. 9, we compare the performance of the three schemes for different numbers of participating nodes  $N_a$ . In particular, in both `Basil+` and `R-plain+`, we have  $N_a = 25G$ , where  $G$  denotes the number of groups, while for `UBAR`, we consider a parallel graph with  $N_a$  nodes. As can be observed from Fig. 9, `Basil+` is not only robust to the Byzantine nodes, but also gives superior performance over `UBAR` in all the 4 cases shown in Fig. 9. The key reason of `Basil+` having higher performance than `UBAR` is that training in `Basil+` includes sequential training over logical rings within groups, which has better performance than graph based decentralized training.

## VII. CONCLUSION AND FUTURE DIRECTIONS

We propose `Basil`, a fast and computationally efficient Byzantine-robust algorithm for decentralized training over a logical ring. We provide the theoretical convergence guarantees of `Basil` demonstrating its linear convergence rate. Our experimental results in the IID setting show the superiority of `Basil` over the state-of-the-art algorithm for decentralized training. Furthermore, we generalize `Basil` to the non-IID

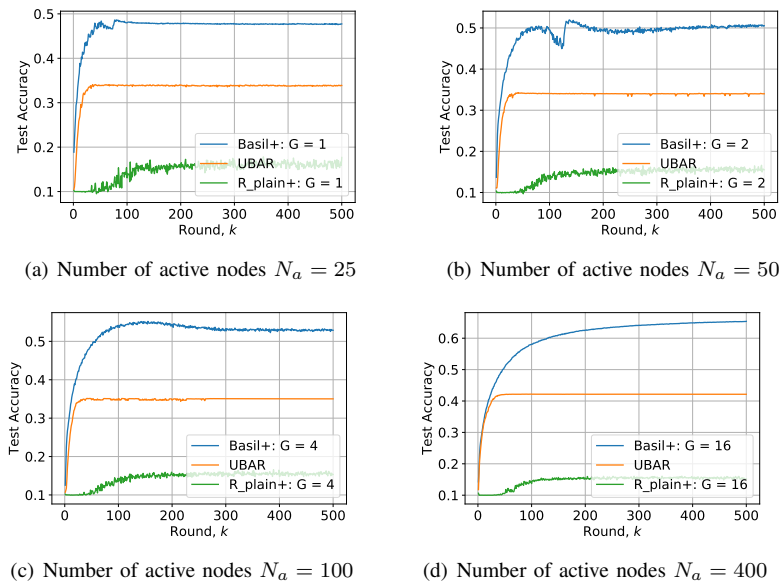


Fig. 9. Illustrating the performance gains of Basil+ over UBAR and R-plain+ for CIFAR10 dataset under different number of nodes  $N_a$ .

setting by integrating it with our proposed Anonymous Cyclic Data Sharing (ACDS) scheme. Finally, we propose Basil+ that enables a parallel implementation of Basil achieving further scalability.

One interesting future direction is to explore some techniques such as data compression or data placement and coded shuffling to reduce the communication cost resulting from using ACDS. Additionally, it is interesting to see how some differential privacy (DP) methods can be adopted by adding noise to the shared data in ACDS to provide further privacy while studying the impact of the added noise in the overall training performance.

## REFERENCES

- [1] J. Devlin, M.-W. Chang, K. Lee, and K. Toutanova, “BERT: Pre-training of deep bidirectional transformers for language understanding,” *North American Chapter of the Association for Computational Linguistics: Human Language Technologies*, pp. 4171–4186, 2019.
- [2] A. Dosovitskiy, L. Beyer, A. Kolesnikov, D. Weissenborn, X. Zhai, T. Unterthiner, M. Dehghani, M. Minderer, G. Heigold, S. Gelly *et al.*, “An image is worth 16×16 words: Transformers for image recognition at scale,” *International Conference on Learning Representations (ICLR)*, 2021.
- [3] E. L. Feld, “United States Data Privacy Law: The Domino Effect After the GDPR,” in *N.C. Banking Inst.*, vol. 24. HeinOnline, 2020, p. 481.
- [4] P. Kairouz, H. B. McMahan, and e. a. Brendan, “Advances and open problems in federated learning,” *preprint arXiv:1912.04977*, 2019.
- [5] X. Lian, C. Zhang, H. Zhang, C.-J. Hsieh, W. Zhang, and J. Liu, “Can decentralized algorithms outperform centralized algorithms? a case study for decentralized parallel stochastic gradient descent,” 2017.
- [6] A. Koloskova, S. Stich, and M. Jaggi, “Decentralized stochastic optimization and gossip algorithms with compressed communication,” in *Proceedings of the 36th International Conference on Machine Learning*, ser. Proceedings of Machine Learning Research, K. Chaudhuri and R. Salakhutdinov, Eds., vol. 97. PMLR, 09–15 Jun 2019, pp. 3478–3487.
- [7] R. Dobbe, D. Fridovich-Keil, and C. Tomlin, “Fully decentralized policies for multi-agent systems: An information theoretic approach,” ser. NIPS’17. Red Hook, NY, USA: Curran Associates Inc., 2017, p. 2945–2954.
- [8] S. Sundhar Ram, A. Nedić, and V. V. Veeravalli, “Asynchronous gossip algorithms for stochastic optimization,” in *Proceedings of the 48th IEEE Conference on Decision and Control (CDC) held jointly with 2009 28th Chinese Control Conference*, 2009, pp. 3581–3586.
- [9] L. Lamport, R. Shostak, and M. Pease, “The byzantine generals problem,” *ACM Trans. Program. Lang. Syst.*, vol. 4, no. 3, p. 382–401, Jul. 1982.
- [10] S. Guo, T. Zhang, H. Yu, X. Xie, L. Ma, T. Xiang, and Y. Liu, “Byzantine-resilient decentralized stochastic gradient descent,” *IEEE Transactions on Circuits and Systems for Video Technology*, pp. 1–1, 2021.
- [11] Z. Yang and W. U. Bajwa, “Bridge: Byzantine-resilient decentralized gradient descent,” *preprint arXiv:1908.08098*, 2019.
- [12] J. Regatti, H. Chen, and A. Gupta, “Bygars: Byzantine sgd with arbitrary number of attackers,” *preprint arXiv:2006.13421*, 2020.
- [13] C. Xie, S. Koyejo, and I. Gupta, “Zeno: Distributed stochastic gradient descent with suspicion-based fault-tolerance,” in *Proceedings of the 36th International Conference on Machine Learning*, ser. Proceedings of Machine Learning Research, K. Chaudhuri and R. Salakhutdinov, Eds., vol. 97. PMLR, 09–15 Jun 2019, pp. 6893–6901.
- [14] —, “Zeno++: Robust fully asynchronous SGD,” in *Proceedings of the 37th International Conference on Machine Learning*, ser. Proceedings of Machine Learning Research, H. D. III and A. Singh, Eds., vol. 119. PMLR, 13–18 Jul 2020, pp. 10495–10503.
- [15] P. Blanchard, E. M. El Mhamdi, R. Guerraoui, and J. Stainer, “Machine learning with adversaries: Byzantine tolerant gradient descent,” in *Proceedings of the 31st International Conference on Neural Information Processing Systems*, ser. NIPS’17. Curran Associates Inc., 2017, p. 118–128.
- [16] D. Yin, Y. Chen, R. Kannan, and P. Bartlett, “Byzantine-robust distributed learning: Towards optimal statistical rates,” in *Proceedings of the 35th International Conference on Machine Learning*, ser. Proceedings of Machine Learning Research, J. Dy and A. Krause, Eds., vol. 80. Stockholm: Stockholm: PMLR, 10–15 Jul 2018, pp. 5650–5659.
- [17] A. R. Elkordy and A. Salman Avestimehr, “Heterosag: Secure aggregation with heterogeneous quantization in federated learning,” *IEEE Transactions on Communications*, pp. 1–1, 2022.
- [18] J. So, B. Güler, and A. S. Avestimehr, “Byzantine-resilient secure federated learning,” *IEEE Journal on Selected Areas in Communications*, 2020.
- [19] K. Pillutla, S. M. Kakade, and Z. Harchaoui, “Robust aggregation for federated learning,” *preprint arXiv:1912.13445*, 2019.
- [20] L. Zhao, S. Hu, Q. Wang, J. Jiang, S. Chao, X. Luo, and P. Hu, “Shielding collaborative learning: Mitigating poisoning attacks through client-side detection,” *IEEE Transactions on Dependable and Secure Computing*, pp. 1–1, 2020.
- [21] S. Prakash, H. Hashemi, Y. Wang, M. Annavaram, and S. Avestimehr, “Byzantine-resilient federated learning with heterogeneous data distribution,” *arXiv preprint arXiv:2010.07541*, 2020.
- [22] T. Zhang, C. He, T.-S. Ma, M. Ma, and S. Avestimehr, “Federated

- learning for internet of things: A federated learning framework for on-device anomaly data detection,” *ArXiv*, vol. abs/2106.07976, 2021.
- [23] E. M. El Mhamdi, R. Guerraoui, and S. Rouault, “The hidden vulnerability of distributed learning in Byzantium,” in *Proceedings of the 35th International Conference on Machine Learning*, ser. Proceedings of Machine Learning Research, J. Dy and A. Krause, Eds., vol. 80. Stockholmsmässan, Stockholm Sweden: PMLR, 10–15 Jul 2018, pp. 3521–3530.
- [24] J. woo Lee, J. Oh, S. Lim, S.-Y. Yun, and J.-G. Lee, “Tornadoaggregate: Accurate and scalable federated learning via the ring-based architecture,” *preprint arXiv:1806.00582*, 2020.
- [25] Y. Zhao, M. Li, L. Lai, N. Suda, D. Civin, and V. Chandra, “Federated learning with non-iid data,” *preprint arXiv:1806.00582*, 2018.
- [26] L. A. Dunning and R. Kresman, “Privacy preserving data sharing with anonymous id assignment,” *IEEE Transactions on Information Forensics and Security*, vol. 8, no. 2, pp. 402–413, 2013.
- [27] M. Castro, B. Liskov, and et al., “Practical byzantine fault tolerance,” *OSDI*, vol. 173–186, 1999.
- [28] A. Krizhevsky, “Learning multiple layers of features from tiny images,” 2009.
- [29] Y. LeCun, C. Cortes, , and C. Burges, “The mnist database of handwritten digits,” <http://yann.lecun.com/exdb/mnist/>, 1998.
- [30] A. Krizhevsky, G. Hinton *et al.*, “Learning multiple layers of features from tiny images,” 2009.

## OVERVIEW

In the following, we summarize the content of the appendix.

- In Appendix A, we prove Propositions 1 and 2.
- In Appendix B, we prove the convergence guarantees of Basil.
- In Appendix C, we describe how Basil can be robust to nodes dropout.
- In Appendix D, Appendix E and Appendix F, the proofs of Propositions 3, 4 and 5 are presented.
- In Appendix G, we present UBAR [10], the recent Byzantine-robust decentralized algorithm.
- In Appendix H, we provide additional experiments.

## APPENDIX A

### PROOF OF PROPOSITION 1 AND PROPOSITION 2

**Proposition 1.** *The communication, computation, and storage complexities of Basil algorithm are all  $\mathcal{O}(Sd)$  for each node in each iteration, where  $d$  is the model size.*

*Proof.* Each node receives and stores the latest  $S$  models, calculates the loss by using each model out of the  $S$  stored models, and multicasts its updated model to the next  $S$  clockwise neighbors. Thus, this results in  $\mathcal{O}(Sd)$  communication, computation, and storage costs.  $\square$

**Proposition 2.** *The number of models that each benign node needs to receive, store and evaluate from its counterclockwise neighbors for ensuring the connectivity and success of Basil can be relaxed to  $S < b+1$  while guaranteeing the success of Basil (benign subgraph connectivity) with high probability.*

*Proof.* This can be proven by showing that the benign subgraph, which is generated by removing the Byzantine nodes, is connected with high probability when each node multicasts its updated model to the next  $S < b+1$  clockwise neighbors instead of  $b+1$  neighbors. Connectivity of the benign subgraph is important as it ensures that each benign node can still receive information from a few other non-faulty nodes. Hence, by letting each node store and evaluate the latest  $S$  model updates, this ensures that each benign node has the chance to select one of the benign updates.

More formally, when each node multicasts its model to the next  $S$  clockwise neighbors, we define  $A_j$  to be the failure event in which  $S$  Byzantine nodes come in a row where  $j$  is the starting node of these  $S$  nodes. When  $A_j$  occurs, there is at least one pair of benign nodes that have no link between them. The probability of  $A_j$  is given as follows:

$$\mathbb{P}(A_j) = \prod_{i=0}^{S-1} \frac{(b-i)}{(N-i)} = \frac{b!(N-S)!}{(b-S)!N!}, \quad (19)$$

where the second equality follows from the definition of factorial, while  $b$ , and  $N$  are the number of Byzantine nodes and the total number of nodes in the system, respectively. Thus, the probability of having a disconnected benign subgraph in Basil, i.e.,  $S$  Byzantine nodes coming in a row, is given as follows:

$$\mathbb{P}(\text{Failure}) = \mathbb{P}\left(\bigcup_{j=1}^N (A_j)\right) \stackrel{(a)}{\leq} \sum_{j=1}^N \mathbb{P}(A_j) \stackrel{(b)}{=} \frac{b!(N-S)!}{(b-S)!(N-1)!}, \quad (20)$$

where (a) follows from the union bound and (b) follows from (19).  $\square$

## APPENDIX B CONVERGENCE ANALYSIS

In this section, we prove the two theorems presented in Section III.B in the main paper. We start the proofs by stating the main assumptions and the update rule of Basil.

**Assumption 1** (IID data distribution). *Local dataset  $\mathcal{Z}_i$  at node  $i$  consists of IID data samples from a distribution  $\mathcal{P}_i$ , where  $\mathcal{P}_i = \mathcal{P}$  for  $i \in \mathcal{R}$ . In other words,  $f_i(\mathbf{x}) = \mathbb{E}_{\zeta_i \sim \mathcal{P}_i} [l(\mathbf{x}, \zeta_i)] = \mathbb{E}_{\zeta_j \sim \mathcal{P}_j} [l(\mathbf{x}, \zeta_j)] = f_j(\mathbf{x}) \forall i, j \in \mathcal{R}$ . Hence, the global loss function  $f(\mathbf{x}) = \mathbb{E}_{\zeta_i \sim \mathcal{P}_i} [l(\mathbf{x}, \zeta_i)]$ .*

**Assumption 2** (Bounded variance). *Stochastic gradient  $g_i(\mathbf{x})$  is unbiased and variance bounded, i.e.,  $\mathbb{E}_{\mathcal{P}_i} [g_i(\mathbf{x})] = \nabla f_i(\mathbf{x}) = \nabla f(\mathbf{x})$ , and  $\mathbb{E}_{\mathcal{P}_i} \|g_i(\mathbf{x}) - \nabla f_i(\mathbf{x})\|^2 \leq \sigma^2$ , where  $g_i(\mathbf{x})$  is the stochastic gradient computed by node  $i$  by using a random sample  $\zeta_i$  from its local dataset  $\mathcal{Z}_i$ .*

**Assumption 3** (Smoothness). *The loss functions  $f'_i$ s are  $L$ -smooth and twice differentiable, i.e., for any  $\mathbf{x} \in \mathbb{R}^d$ , we have  $\|\nabla^2 f_i(\mathbf{x})\|_2 \leq L$ .*

Let  $b^i$  be the number of Byzantine nodes out of the  $S$  counterclockwise neighbors of node  $i$ . We divide the set of stored models  $\mathcal{N}_k^i$  at node  $i$  in the  $k$ -th round into two sets. The first set  $\mathcal{G}_k^i = \{\mathbf{y}_1, \dots, \mathbf{y}_{r^i}\}$  contains the benign models, where  $r^i = S - b^i$ . We consider scenarios with  $S = b + 1$ , where  $b$  is the total number of Byzantine nodes in the network. Without loss of generality, we assume the models in this set are arranged such that the first model is from the closest benign node in the neighborhood of node  $i$ , while the last model is from the farthest node. Similarly, we define the second set  $\mathcal{B}_k^i$  to be the set of models from the counterclockwise Byzantine neighbors of node  $i$  such that  $\mathcal{B}_k^i \cup \mathcal{G}_k^i = \mathcal{N}_k^i$ .

The general update rule in Basil is given as follows. At the  $k$ -th round, the current active node  $i$  updates the global model according to the following rule:

$$\mathbf{x}_k^{(i)} = \bar{\mathbf{x}}_k^{(i)} - \eta_k^{(i)} g_i(\bar{\mathbf{x}}_k^{(i)}), \quad (21)$$

where  $\bar{\mathbf{x}}_k^{(i)}$  is given as follows

$$\bar{\mathbf{x}}_k^{(i)} = \arg \min_{\mathbf{y} \in \mathcal{N}_k^i} \mathbb{E} [l_i(\mathbf{y}, \zeta_i)]. \quad (22)$$

### A. Proof of Theorem 1

We first show that if node  $i$  completed the performance-based criteria in (22) and selected the model  $\mathbf{y}_1 \in \mathcal{G}_k^i$ , and updated its model as follows:

$$\mathbf{x}_k^{(i)} = \mathbf{y}_1 - \eta_k^{(i)} g_i(\mathbf{y}_1), \quad (23)$$

we will have

$$\mathbb{E} [\ell_{i+1}(\mathbf{x}_k^{(i)})] \leq \mathbb{E} [\ell_{i+1}(\mathbf{y}_1)], \quad (24)$$

where  $\ell_{i+1}(\mathbf{y}_1) = \ell_{i+1}(\mathbf{y}_1, \zeta_{i+1})$  is the loss function of node  $i+1$  evaluated on a random sample  $\zeta_{i+1}$  by using the model  $\mathbf{y}_1$ .

The proof of (24) is as follows: By using Taylor's theorem, there exists a  $\gamma$  such that

$$\begin{aligned} \ell_{i+1}(\mathbf{x}_k^{(i)}) &= \ell_{i+1}(\mathbf{y}_1 - \eta_k^{(i)} g_i(\mathbf{y}_1)) \\ &= \ell_{i+1}(\mathbf{y}_1) - \eta_k^{(i)} g_i(\mathbf{y}_1)^T g_{i+1}(\mathbf{y}_1) \\ &\quad + \frac{1}{2} \eta_k^{(i)2} g_i(\mathbf{y}_1)^T \nabla^2 \ell_{i+1}(\gamma) \eta_k^{(i)} g_i(\mathbf{y}_1), \end{aligned} \quad (25)$$

where  $\nabla^2 \ell_{i+1}$  is the stochastic Hessian matrix. By using the following assumption

$$\|\nabla^2 \ell_{i+1}(\mathbf{x}_k^{(i)})\|_2 \leq L, \quad (27)$$

for all random samples  $\zeta_{i+1}$  and any model  $\mathbf{x} \in \mathbb{R}^d$ , where  $L$  is the Lipschitz constant, we get

$$\begin{aligned} \ell_{i+1}(\mathbf{x}_k^{(i)}) &\leq \ell_{i+1}(\mathbf{y}_1) - \eta_k^{(i)} g_i(\mathbf{y}_1)^T g_{i+1}(\mathbf{y}_1) \\ &\quad + \frac{(\eta_k^{(i)})^2 L}{2} \|g_i(\mathbf{y}_1)\|^2. \end{aligned} \quad (28)$$

By taking the expected value of both sides of this expression (where the expectation is taken over the randomness in the sample selection), we get

$$\begin{aligned} &\mathbb{E} [\ell_{i+1}(\mathbf{x}_k^{(i)})] \leq \mathbb{E} [\ell_{i+1}(\mathbf{y}_1)] - \eta_k^{(i)} \mathbb{E} [g_i(\mathbf{y}_1)^T g_{i+1}(\mathbf{y}_1)] \\ &\quad + \frac{(\eta_k^{(i)})^2 L}{2} \mathbb{E} \|g_i(\mathbf{y}_1)\|^2 \\ &\stackrel{a}{=} \mathbb{E} [\ell_{i+1}(\mathbf{y}_1)] - \eta_k^{(i)} \mathbb{E} [g_i(\mathbf{y}_1)^T] \mathbb{E} [g_{i+1}(\mathbf{y}_1)] \\ &\quad + \frac{(\eta_k^{(i)})^2 L}{2} \mathbb{E} \|g_i(\mathbf{y}_1)\|^2 \\ &\leq \mathbb{E} [\ell_{i+1}(\mathbf{y}_1)] - \eta_k^{(i)} \mathbb{E} [g_i(\mathbf{y}_1)^T] \mathbb{E} [g_{i+1}(\mathbf{y}_1)] \\ &\quad + (\eta_k^{(i)})^2 L \mathbb{E} \|g_i(\mathbf{y}_1)\|^2 \\ &\stackrel{b}{\leq} \mathbb{E} [\ell_{i+1}(\mathbf{y}_1)] - \eta_k^{(i)} \|\nabla f(\mathbf{y}_1)\|^2 + (\eta_k^{(i)})^2 L \|\nabla f(\mathbf{y}_1)\|^2 \\ &\quad + (\eta_k^{(i)})^2 L \sigma^2 \\ &= \mathbb{E} [\ell_{i+1}(\mathbf{y}_1)] - \|\nabla f(\mathbf{y}_1)\|^2 \left( \eta_k^{(i)} - (\eta_k^{(i)})^2 L \right) + (\eta_k^{(i)})^2 L \sigma^2, \end{aligned} \quad (29)$$

where (a) follows from that the samples are drawn from independent data distribution, while (b) from Assumption 1 along with

$$\begin{aligned} \mathbb{E} \|g_i(\mathbf{y}_1)\|^2 &= \mathbb{E} \|g_i(\mathbf{y}_1) - \mathbb{E} [g_i(\mathbf{y}_1)]\|^2 + \|\mathbb{E} [g_i(\mathbf{y}_1)]\|^2 \\ &\leq \sigma^2 + \|\nabla f(\mathbf{y}_1)\|^2. \end{aligned} \quad (30)$$

Let  $C_k^i = \frac{\|\nabla f(\mathbf{y}_1)\|^2}{\|\nabla f(\mathbf{y}_1)\|^2 + \sigma^2} = \frac{\|\mathbb{E} [g_i(\mathbf{y}_1)]\|^2}{\|\mathbb{E} [g_i(\mathbf{y}_1)]\|^2 + \sigma^2}$ , which implies that  $C_k^i \in [0, 1]$ . By selecting the learning rate as  $\eta_k^{(i)} \geq \frac{1}{L} C_k^i$ , we get

$$\mathbb{E} [\ell_{i+1}(\mathbf{y}_1)] \leq \mathbb{E} [\ell_{i+1}(\mathbf{y}_1)]. \quad (31)$$

Note that, nodes can just use a learning rate  $\eta \geq \frac{1}{L}$ , since  $C_k^i \in [0, 1]$ , while still achieving (31). This completes the first part of the proof.

By using (31), it can be easily seen that the update rule in equation (21) can be reduced to the case where each node updates its model based on the model received from the closest benign node (23) in its neighborhood, where this follows from using induction.

Let's consider this example. Consider a ring with  $N$  nodes and by using  $S = 3$  while ignoring the Byzantine nodes for a while (assume all nodes are benign nodes). We consider the first round  $k = 1$ . With a little abuse of notations, we can get the following, the updated model by node 1 (the first node in the ring)  $\mathbf{x}_1 = h(\mathbf{x}_0)$  is a function of the initial model  $\mathbf{x}_0$  (updated by using the model  $\mathbf{x}_0$ ). Now, node 2 has to select one model from the set of two models  $\mathcal{N}_k^2 = \{\mathbf{x}_1 = h(\mathbf{x}_0), \mathbf{x}_0\}$ . The selection is performed by evaluating the expected loss function of node 2 by using the criteria given in (22) on the models on the set  $\mathcal{N}_k^2$ . According to (31), node 2 will select the model  $\mathbf{x}_1$  which results in lower expected loss. Now, node 2 updates its model based on the model  $\mathbf{x}_1$ , i.e.,  $\mathbf{x}_2 = h(\mathbf{x}_1)$ . After that, node 3 applies the aggregation rule in (22) to select one model from this set of models  $\mathcal{N}_k^3 = \{\mathbf{x}_2 = h(\mathbf{x}_1), \mathbf{x}_1 = h(\mathbf{x}_0), \mathbf{x}_0\}$ . By using (31) and Assumption 1, we get

$$\mathbb{E} [\ell_3(\mathbf{x}_2)] \leq \mathbb{E} [\ell_3(\mathbf{x}_1)] \leq \mathbb{E} [\ell_3(\mathbf{x}_0)], \quad (32)$$

and node 3 model will be updated according to the model  $\mathbf{x}_2$ , i.e.,  $\mathbf{x}_3 = h(\mathbf{x}_2)$ .

More generally, the set of stored benign models at node  $i$  is given by  $\mathcal{N}_k^i = \{\mathbf{y}_1 = h(\mathbf{y}_2), \mathbf{y}_2 = h(\mathbf{y}_3), \dots, \mathbf{y}_{r^i} = h(\mathbf{y}_{r^{i-1}})\}$ , where  $r^i$  is the number of benign models in the set  $\mathcal{N}_k^i$ . According to (31), we will have the following

$$\mathbb{E} [l_i(\mathbf{y}_1)] \leq \mathbb{E} [l_i(\mathbf{y}_2)] \leq \dots \leq \mathbb{E} [l_i(\mathbf{y}_{r^i})] \leq \mathbb{E} [l_i(\mathbf{x})] \quad \forall \mathbf{x} \in \mathcal{B}_k^i, \quad (33)$$

where the last inequality in (33) follows from the fact that the Byzantine nodes are sending faulty models and their expected loss is supposed to be higher than the expected loss of the benign nodes.

According to this discussion and by removing the Byzantine nodes thanks to (33), we can only consider the benign subgraph which is generated by removing the Byzantine nodes according to the discussion in Section III-A in the main paper. Note that by letting each active node send its updated model to the next  $b+1$  nodes, where  $b$  is the total number of Byzantine nodes, the benign subgraph can always be connected. By



considering the benign subgraph (the logical rings without Byzantine nodes), we assume without loss of generality that the indices of benign nodes in the ring are arranged in ascending order starting from node 1 to node  $r$ . In this benign subgraph, the update rule will be given as follows

$$\mathbf{x}_k^{(i)} = \mathbf{x}_k^{(i-1)} - \eta_k^{(i)} g_i(\mathbf{x}_k^{(i-1)}). \quad (34)$$

### B. Proof of Theorem 2

By using Taylor's theorem, there exists a  $\gamma$  such that

$$\begin{aligned} f(\mathbf{x}_k^{(i+1)}) &\stackrel{a}{=} f\left(\mathbf{x}_k^{(i)} - \eta_k^{(i+1)} g_{i+1}(\mathbf{x}_k^{(i)})\right) \\ &= f(\mathbf{x}_k^{(i)}) - \eta_k^{(i+1)} \left(g_{i+1}(\mathbf{x}_k^{(i)})\right)^T \nabla f(\mathbf{x}_k^{(i)}) \\ &\quad + \frac{1}{2} \eta_k^{(i+1)} \left(g_{i+1}(\mathbf{x}_k^{(i)})\right)^T \nabla^2 f(\gamma) \eta_k^{(i+1)} g_{i+1}(\mathbf{x}_k^{(i)}) \\ &\stackrel{b}{\leq} f(\mathbf{x}_k^{(i)}) - \eta_k^{(i+1)} \left(g_{i+1}(\mathbf{x}_k^{(i)})\right)^T \nabla f(\mathbf{x}_k^{(i)}) \\ &\quad + \frac{L}{2} \eta_k^{(i+1)} \|g_{i+1}(\mathbf{x}_k^{(i)})\|^2, \end{aligned} \quad (35)$$

where (a) follows from the update rule in (34), while  $f$  is the global loss function in equation (1) in the main paper, and (b) from Assumption 3 where  $\|\nabla^2 f(\gamma)\| \leq L$ . Given the model  $\mathbf{x}_k^{(i)}$ , we take expectation over the randomness in selection of sample  $\zeta_{i+1}$  (the random sample used to get the model  $\mathbf{x}_k^{(i+1)}$ ). We recall that  $\zeta_{i+1}$  is drawn according to the distribution  $\mathcal{P}_{i+1}$  and is independent of the model  $\mathbf{x}_k^{(i)}$ . Therefore, we get the following set of equations:

$$\begin{aligned} \mathbb{E}[f(\mathbf{x}_k^{(i+1)})] &\leq f(\mathbf{x}_k^{(i)}) - \eta_k^{(i)} \mathbb{E}\left[\left(g_{i+1}(\mathbf{x}_k^{(i)})\right)^T \nabla f(\mathbf{x}_k^{(i)})\right] \\ &\quad + \frac{(\eta_k^{(i)})^2 L}{2} \mathbb{E}\|g_{i+1}(\mathbf{x}_k^{(i)})\|^2 \\ &\stackrel{a}{\leq} f(\mathbf{x}_k^{(i)}) - \eta_k^{(i)} \|\nabla f(\mathbf{x}_k^{(i)})\|^2 + \frac{(\eta_k^{(i)})^2 L}{2} \|\nabla f(\mathbf{x}_k^{(i)})\|^2 \\ &\quad + \frac{(\eta_k^{(i)})^2 L}{2} \sigma^2 \\ &= f(\mathbf{x}_k^{(i)}) - \|\nabla f(\mathbf{x}_k^{(i)})\|^2 \left(\eta_k^{(i)} - \frac{(\eta_k^{(i)})^2 L}{2}\right) \\ &\quad + \frac{(\eta_k^{(i)})^2 L}{2} \sigma^2 \\ &\stackrel{b}{\leq} f(\mathbf{x}_k^{(i)}) - \frac{\eta_k^{(i)}}{2} \|\nabla f(\mathbf{x}_k^{(i)})\|^2 + \frac{\eta_k^{(i)}}{2} \sigma^2, \end{aligned} \quad (36)$$

where (a) follows from (30), and (b) by selecting  $\eta_k^{(i)} \leq \frac{1}{L}$ . Furthermore, in the proof of Theorem 1, we choose the learning to be  $\eta_k^{(i)} \geq \frac{1}{L}$ . Therefore, the learning rate will be given by  $\eta_k^{(i)} = \frac{1}{L}$ . By the convexity of the loss function  $f$ , we get the next inequality from the inequality in (36)

$$\begin{aligned} \mathbb{E}[f(\mathbf{x}_k^{(i+1)})] &\leq f(\mathbf{x}^*) + \langle \nabla f(\mathbf{x}_k^{(i)}), \mathbf{x}_k^{(i)} - \mathbf{x}^* \rangle \\ &\quad - \frac{\eta_k^{(i)}}{2} \|\nabla f(\mathbf{x}_k^{(i)})\|^2 + \frac{\eta_k^{(i)}}{2} \sigma^2. \end{aligned} \quad (37)$$

We now back-substitute  $g_i(\mathbf{x}_k^{(i)})$  into (37) by using  $\mathbb{E}[g_{i+1}(\mathbf{x}_k^{(i)})] = \nabla f(\mathbf{x}_k^{(i)})$  and  $\|\nabla f(\mathbf{x}_k^{(i)})\|^2 \geq \mathbb{E}\|g_{i+1}(\mathbf{x}_k^{(i)})\|^2 - \sigma^2$ :

$$\begin{aligned} \mathbb{E}[f(\mathbf{x}_k^{(i+1)})] &\leq f(\mathbf{x}^*) + \langle \mathbb{E}[g_{i+1}(\mathbf{x}_k^{(i)})], \mathbf{x}_k^{(i)} - \mathbf{x}^* \rangle \\ &\quad - \frac{\eta_k^{(i)}}{2} \mathbb{E}\|g_{i+1}(\mathbf{x}_k^{(i)})\|^2 + \eta_k^{(i)} \sigma^2 \\ &= f(\mathbf{x}^*) + \mathbb{E}[\langle [g_{i+1}(\mathbf{x}_k^{(i)})], \mathbf{x}_k^{(i)} - \mathbf{x}^* \rangle] \\ &\quad - \frac{\eta_k^{(i)}}{2} \mathbb{E}\|g_{i+1}(\mathbf{x}_k^{(i)})\|^2 + \eta_k^{(i)} \sigma^2. \end{aligned} \quad (38)$$

By completing the square of the middle two terms to get:

$$\begin{aligned} \mathbb{E}[f(\mathbf{x}_k^{(i+1)})] &\leq f(\mathbf{x}^*) \\ &\quad + \mathbb{E}\left[\frac{1}{2\eta_k^{(i)}} \left(\|\mathbf{x}_k^{(i)} - \mathbf{x}^*\|^2 - \|\mathbf{x}_k^{(i)} - \mathbf{x}^* - \eta_k^{(i)} g_{i+1}(\mathbf{x}_k^{(i)})\|^2\right)\right] \\ &\quad + \eta_k^{(i)} \sigma^2. \\ &= f(\mathbf{x}^*) + \mathbb{E}\left[\frac{1}{2\eta_k^{(i)}} \left(\|\mathbf{x}_k^{(i)} - \mathbf{x}^*\|^2 - \|\mathbf{x}_k^{(i+1)} - \mathbf{x}^*\|^2\right)\right] \\ &\quad + \eta_k^{(i)} \sigma^2. \end{aligned} \quad (39)$$

For  $K$  rounds and  $r$  benign nodes, we note that the total number of SGD steps are  $T = Kr$ . We let  $s = kr + i$  represent the number of updates happen to the initial model  $\mathbf{x}^0$ , where  $i = 1, \dots, r$  and  $k = 0, \dots, K-1$ . Therefore,  $\mathbf{x}_k^{(i)}$  can be written as  $\mathbf{x}^s$ . With the modified notation, we can now take the expectation in the above expression over the entire sampling process during training and then by summing the above equations for  $s = 0, \dots, T-1$ , while taking  $\eta = \frac{1}{L}$ , we have the following:

$$\begin{aligned} &\sum_{s=0}^{T-1} (\mathbb{E}[f(\mathbf{x}^{s+1})] - f(\mathbf{x}^*)) \\ &\leq \frac{L}{2} \left(\|\mathbf{x}^0 - \mathbf{x}^*\|^2 - \mathbb{E}\|\mathbf{x}_k^{(T)} - \mathbf{x}^*\|^2\right) + \frac{1}{L} T \sigma^2. \end{aligned} \quad (40)$$

By using the convexity of  $f(\cdot)$ , we get

$$\begin{aligned} \mathbb{E}\left[f\left(\frac{1}{T} \sum_{s=1}^T \mathbf{x}^s\right)\right] - f(\mathbf{x}^*) &\leq \frac{1}{T} \sum_{s=0}^{T-1} \mathbb{E}[f(\mathbf{x}^{s+1})] - f(\mathbf{x}^*) \\ &\leq \frac{\|\mathbf{x}^0 - \mathbf{x}^*\|^2 L}{2T} + \frac{1}{L} \sigma^2. \end{aligned} \quad (41)$$

## APPENDIX C JOINING AND LEAVING OF NODES

Basil can handle the scenario of 1) node dropouts out of the  $N$  available nodes 2) nodes rejoining the system.

### A. Nodes Dropout

For handling node dropouts, we allow for extra communication between nodes. In particular, each active node can multicast its model to the  $S=b+d+1$  clockwise neighbors, where  $b$  and  $d$  are respectively the number of Byzantine nodes and the worst case number of dropped nodes, and each node can store only the latest  $b+1$  model updates. By doing that,

each benign node will have at least 1 benign update even in the worst case where all Byzantine nodes appear in a row and  $d$  (out of  $S$ ) counterclockwise nodes drop out.

### B. Nodes Rejoining

To address a node *rejoining* the system, this rejoined node can re-multicast its ID to all other nodes. Since benign nodes know the correct order of the nodes (IDs) in the ring according to Section III-A, each active node out of the  $L=b+d+1$  counterclockwise neighbors of the rejoined node sends its model to it, and this rejoined node stores the latest  $b+1$  models. We note that handling participation of new fresh nodes during training is out of scope of our paper, as we consider mitigating Byzantine nodes in decentralized training with a *fixed* number of  $N$  nodes

#### APPENDIX D PROOF OF PROPOSITION 3

We first prove the communication cost given in Proposition 3, which corresponds to node  $1_g$ , for  $g \in [G]$ . We recall from Section IV that in ACDS, each node  $i \in \mathcal{N}$  has  $H$  batches each of size  $\frac{\alpha D}{H}$  data points. Furthermore, for each group  $g \in [G]$ , the anonymous cyclic data sharing phase (phase 2) consists of  $H+1$  rounds. The communication cost of node  $1_g$  in the first round is  $\frac{\alpha D}{H}I$  bits, where  $\frac{\alpha D}{H}$  is the size of one batch and  $I$  is the size of one data point in bits. The cost of each round  $h \in [2, H+1]$  is  $n\frac{\alpha D}{H}I$ , where node  $1_g$  sends the set of shuffled data from the  $n$  batches  $\{c_{1_g}^h, c_{2_g}^{h-1}, \dots, c_{n_g}^{h-1}\}$  to node  $2_g$ . Hence, the total communication cost for node  $1_g$  in this phase is given by  $C_{\text{ACDS}}^{\text{phase-2}} = \alpha DI(\frac{1}{H} + n)$ . In phase 3, node  $1_g$  multicasts its set of shuffled data from batches  $\{c_{1_g}^h, c_{2_g}^h, \dots, c_{n_g}^h\}_{h \in [H]}$  to all nodes in the other groups at a cost of  $n\alpha DI$  bits. Finally, node  $1_g$  receives  $(G-1)$  set of batches  $\{c_{1_{g'}}^h, c_{2_{g'}}^h, \dots, c_{n_{g'}}^h\}_{h \in [H], g' \in [G] \setminus \{g\}}$  at a cost of  $(G-1)n\alpha DI$ . Hence, the communication cost of the third phase of ACDS is given by  $C_{\text{ACDS}}^{\text{phase-3}} = \alpha DnGI$ . By adding the cost of Phase 2 and Phase 3, we get the first result in Proposition 3.

Now, we prove the communication time of ACDS by first computing the time needed to complete the anonymous data sharing phase (phase-2), and then compute the time for the multicasting phase. The second phase of ACDS consists of  $H+1$  rounds. The communication time of the first round is given by  $T_{R_1} = \sum_{i=1}^n iT$ , where  $n$  is the number of nodes in each group. Here,  $T = \frac{\alpha DI}{HR}$  is the time needed to send one batch of size  $\frac{\alpha DI}{H}$  data points with  $R$  being the communication bandwidth in b/s, and  $I$  is the size of one data points in bits. On the other hand, the time for each round  $h \in [2, H]$ , is given by  $T_{R_h} = n^2T$ , where each node sends  $n$  batches. Finally, the time for completing the dummy round, the  $(H+1)$ -th round, is given by  $T_{R_{H+1}} = n(n-2)T$  where only the first  $n-2$  nodes in the ring participate in this round as discussed in Section IV. Therefore, the total time for completing the anonymous cyclic data sharing phase (phase 2 of ACDS) is given by  $T_{\text{phase-2}} = T_{R_1} + (H-1)T_{R_h} + T_{R_{H+1}} = T(n^2(H+0.5) - 1.5n)$  as this phase happens in parallel for all the  $G$  groups. The time for completing the multicasting phase is  $T_{\text{phase-3}} = (G-1)nHT$ ,

where each node in group  $g$  receives  $nH$  batches from each node  $1_{g'} \in [G] \setminus \{g\}$ . By adding  $T_{\text{phase-2}}$  and  $T_{\text{phase-3}}$ , we get the communication time of ACDS given in Proposition 3.

#### APPENDIX E PROOF OF PROPOSITION 4

We recall from Section III that the per round training time of `Basil` is divided into four parts. In particular, each active node (1) receives the model from the  $S$  counterclockwise neighbors; (2) evaluates the  $S$  models using the `Basil` aggregation rule; (3) updates the model by taking one step of SGD; and (4) multicasts the model to the next  $S$  clockwise neighbors.

Assuming training begins at time 0, we define  $E_i^{(k)}$  to be the wall-clock time at which node  $i$  finishes the training in round  $k$ . We also define  $T_{\text{com}} = \frac{32d}{R}$  to be the time to receive one model of size  $d$  elements each of size 32 bits, where each node receives only one model at each step in the ring as the training is sequential. Furthermore, we let  $T_{\text{comp}} = T_{\text{perf-based}} + T_{\text{SGD}}$  to be the time needed to evaluate  $S$  models and perform one step of SGD update.

We assume that each node  $i \in \mathcal{N}$  becomes active and starts evaluating the  $S$  models (using (3)) and taking the SGD model update step (using (2)) only when it receives the model from its counter clock-wise neighbor. Therefore, for the first round, we have the following time recursion:

$$E_1^{(1)} = T_{\text{SGD}} \quad (42)$$

$$E_n^{(1)} = E_{n-1}^{(1)} + T_{\text{com}} + (n-1)T_{\text{perf-based}} + T_{\text{SGD}} \text{ for } n \in [2, S] \quad (43)$$

$$E_n^{(1)} = E_{n-1}^{(1)} + T_{\text{com}} + T_{\text{comp}} \text{ for } n \in [S+1, N], \quad (44)$$

where (42) follows from the fact that node 1 just takes one step of model update using the initial model  $\mathbf{x}^0$ . Each node  $i \in [2, S]$  receives the model from its own node, evaluates the  $(i-1)$  received model and then takes one step of model update. For node  $i \in [S+1, N]$ , each node will have  $S$  models to evaluate, and the time recursion follows (44).

The time recursions, for the remaining  $\tau$  rounds, where the training is assumed to happen over  $\tau$  rounds, are given by

$$E_1^{(k+1)} = E_n^{(k)} + T_{\text{com}} + T_{\text{comp}} \text{ for } k \in [\tau-1] \quad (45)$$

$$E_n^{(k)} = E_{n-1}^{(k)} + T_{\text{com}} + T_{\text{comp}} \text{ for } n \in [N] \setminus \{1\}, k \in [\tau] \quad (46)$$

$$E_1^{(\tau+1)} = E_n^{(\tau)} + T_{\text{com}} + ST_{\text{perf-based}}. \quad (47)$$

By telescoping (42)-(47), we get the upper bound in (15).

The training time of `Basil+` in (16) can be proven by computing the time of each stage of the algorithm: In Stage 1, all groups in parallel apply `Basil` algorithm within its group, where the training is carried out sequentially. This results in a training time of  $T_{\text{stage1}} \leq n\tau T_{\text{perf-based}} + n\tau T_{\text{comm}} + n\tau T_{\text{SGD}}$ . The time of the robust circular aggregation stage is given by  $T_{\text{stage2}} = GT_{\text{perf-based}} + SGT_{\text{comm}}$ . Here,  $ST_{\text{perf-based}}$  in the first term comes from the fact that each node in the set  $S_g$  in

parallel evaluates  $S$  models received from the nodes in  $\mathcal{S}_{g-1}$ . The second term in  $T_{\text{stage2}}$  comes from the fact that each node in  $\mathcal{S}_g$  receives  $S$  models from the nodes in  $\mathcal{S}_{g-1}$ . The term  $G$  in stage 2 results from the sequential aggregation over the  $G$  groups. The time of the final stage (multicasting stage) is given by  $T_{\text{stage3}} = T_{\text{perf-based}} + (G-1)T_{\text{comm}}$ , where the first term from the fact all nodes in the set  $\{\mathcal{U}_1, \mathcal{U}_2, \dots, \mathcal{U}_{G-1}\}$  evaluates the  $S$  robust average model in parallel, while the second term follows from the time needed to receive the  $S$  robust average model by each corresponding node in the remaining groups. By combining the time of the three stages, we get the training time given in (16).

## APPENDIX F PROOF OF PROPOSITION 5

**Proposition 5.** *The connectivity parameter  $S$  in Basil+ can be relaxed to  $S < n - 1$  while guaranteeing the success of the algorithm (benign local/global subgraph connectivity) with high probability. The failure probability of Basil+ is given by*

$$\mathbb{P}(F) \leq G \sum_{i=0}^{\min(b,n)} \left( \prod_{s=0}^{S-1} \frac{\max(i-s, 0)}{(N-s)} n \right) \frac{\binom{b}{i} \binom{N-b}{n-i}}{\binom{N}{n}}, \quad (48)$$

where  $N$ ,  $n$ ,  $G$ ,  $S$  and  $b$  are the number of total nodes, number of nodes in each group, number of groups, the connectivity parameter, and the number of Byzantine nodes.

*Proof.* At a high level, Basil+ would fail if at least one group out of the  $G$  groups failed (the set of models  $\mathcal{L}_g$  sent from the set  $\mathcal{S}_g$  in any particular group  $g$  to the group  $g+1$  are faulty). According to the discussion in the proof of proposition 2, group  $g$  fails, when we  $S$  Byzantine nodes comes in a row.

Now, we formally prove the failure probability of Basil+. We start our proof by defining the failure event of Basil+ by

$$F = \bigcup_{g=1}^G F_g, \quad (49)$$

where  $F_g$  is the failure event of group  $g$  and  $G$  is the number of groups. The failure probability of group  $g$  is given by

$$\mathbb{P}(F_g) = \sum_{i=0}^{\min(b,n)} \mathbb{P}(F_g \mid b_g = i) \mathbb{P}(b_g = i), \quad (50)$$

where  $b_g$  is the number of Byzantine nodes in group  $g$ . Equation (50) follows the law of total probability. The conditional probability in (50) represents the failure probability of group  $g$  given  $i$  nodes in that group are Byzantine nodes. This conditional group failure probability can be derived similarly to the failure probability in (20) in Proposition 2. In particular, the conditional probability is formally given by

$$\mathbb{P}(F_g \mid b_g = i) \leq \sum_{j=1}^n \mathbb{P}(A_j \mid b_g = i), \quad (51)$$

where  $A_j$  is the failure event in which  $S$  Byzantine nodes come in a row, where  $j$  is the starting node of these  $S$  nodes

given that there are  $i$  Byzantine nodes in that group. The probability  $\mathbb{P}(A_j \mid b_g = i)$  is given as follows

$$\mathbb{P}(A_j \mid b_g = i) = \prod_{s=0}^{S-1} \frac{\max(i-s, 0)}{(N-s)}, \quad (52)$$

where  $i$  is the number of Byzantine nodes in group  $g$  and  $S$  is the connectivity parameter in that group. By combining (52) with (51), we get the conditional probability in the first term in (50) which is given as follows

$$\mathbb{P}(F_g \mid b_g = i) \leq \sum_{j=1}^n \mathbb{P}(A_j \mid b_g = i) = \prod_{s=0}^{S-1} \frac{\max(i-s, 0)}{(N-s)} n. \quad (53)$$

The probability  $\mathbb{P}(b_g = i)$  in the second term of (50) follows a Hypergeometric distribution with parameter  $(N, b, n)$  where  $N$ ,  $b$ , and  $n$  are the total number of nodes, total number of Byzantine nodes, number of nodes in each group, respectively. This probability is given by

$$\mathbb{P}(b_g = i) = \frac{\binom{b}{i} \binom{N-b}{n-i}}{\binom{N}{n}}. \quad (54)$$

By substituting (54) and (53) in (50), we get the failure probability of one group in Basil+, which is given as follows

$$\mathbb{P}(F_g) \leq \sum_{i=0}^{\min(b,n)} \left( \prod_{s=0}^{S-1} \frac{\max(i-s, 0)}{(N-s)} n \right) \frac{\binom{b}{i} \binom{N-b}{n-i}}{\binom{N}{n}}. \quad (55)$$

Finally, the failure probability of Basil+ is given by

$$\begin{aligned} \mathbb{P}(F) &= \mathbb{P}\left(\bigcup_{g=1}^G F_g\right) \\ &\stackrel{(a)}{\leq} \sum_{g=1}^G \mathbb{P}(F_g) \\ &= G \sum_{i=0}^{\min(b,n)} \left( \prod_{s=0}^{S-1} \frac{\max(i-s, 0)}{(N-s)} n \right) \frac{\binom{b}{i} \binom{N-b}{n-i}}{\binom{N}{n}}, \end{aligned} \quad (56)$$

where (a) follows the union bound.  $\square$

## APPENDIX G UBAR

In this section, we describe UBAR [10], the SOTA Byzantine resilient approach for parallel decentralized training.

### A. Algorithm

This decentralized training setup is defined over undirected graph:  $\mathcal{G} = (V, E)$ , where  $V$  denotes a set of  $N$  nodes and  $E$  denotes a set of edges representing communication links. Filtering Byzantine nodes is done over two stages for each training iteration. At the first stage, each benign node performs a distance-based strategy to select a candidate pool of potential benign nodes from its neighbors. This selection is performed by comparing the Euclidean distance of its own model with the model from its neighbors. In the second stage, each benign node performs a performance-based strategy to pick the final

nodes from the candidate pool resulted from stage 1. It reuses the training sample as the validation data to compute the loss function value of each model. It selects the models whose loss values are smaller than the value of its own model, and calculates the average of those models as the final updated value. Formally, the update rule in UBAR is given by

$$\mathbf{x}_{k+1}^{(i)} = \alpha \mathbf{x}_k^{(i)} + (1 - \alpha) \mathcal{R}_{\text{UBAR}}(\mathbf{x}_k^{(j)}, j \in \mathcal{N}_i) - \eta \nabla f_i(\mathbf{x}_k^{(i)}), \quad (57)$$

where  $\mathcal{N}_i$  is the set of neighbors of Node  $i$ ,  $\nabla f_i(\mathbf{x}_k^{(i)})$  is the local gradient of node  $i$  evaluated on a random sample from the local dataset of node  $i$  while using its own model,  $k$  is the training round, and  $\mathcal{R}_{\text{UBAR}}$  is given as follows:

$$\mathcal{R}_{\text{UBAR}} = \begin{cases} \frac{1}{N_{i,k}^r} \sum_{j \in \mathcal{N}_{i,k}^r} \mathbf{x}_k^{(j)} & \text{if } \mathcal{N}_{i,k}^r \neq \phi \\ \mathbf{x}_k^j & \text{Otherwise,} \end{cases} \quad (58)$$

where there are two stages of filtering:

$$(1) \mathcal{N}_{i,k}^s = \arg \min_{\substack{\mathcal{N}^* \subset \mathcal{N}_i \\ |\mathcal{N}^*| = \rho_i |\mathcal{N}_i|}} \sum_{j \in \mathcal{N}_i} \|\mathbf{x}_k^{(j)} - \mathbf{x}_k^{(i)}\|,$$

$$(2) \mathcal{N}_{i,k}^r = \bigcup_{j \in \mathcal{N}_{i,k}^s} j, \text{ and } j^* = \arg \min_{j \in \mathcal{N}_{i,k}^s} \ell_i(\mathbf{x}_k^{(j)}).$$

$$\ell_i(\mathbf{x}_k^{(j)}) \leq \ell_i(\mathbf{x}_k^{(i)})$$

### B. Time Analysis for UBAR

The training time of UBAR is divided into two parts; computation time and communication time. We start by discussing the communication time. For modeling the communication time, we assume that each node in parallel can multicast its model to its neighbors and receive the models from the neighbor nodes, where each node is assumed to be connected to  $S$  neighbors. Hence, the time to multicast  $S$  models can be calculated as  $\frac{d32}{R}$ , where  $d$  is the model size and each element of the model is represented by 32 bits and  $R$  is the communication BW in b/s. On the other hand, the time to receives  $S$  different models from the  $S$  neighbor nodes is given by  $\frac{S*d*32}{R}$ . We assume that in UBAR, each node starts the model evaluations and model update after receiving the  $S$  models (the same assumption is used when computing the training time for Basil). Therefore, given that each node starts the training procedure only when it receives the  $S$  models while all the communications happen in parallel in the graph, the communication time in one parallel round in UBAR is given as follows:

$$T_{\text{UBAR-communication}} = \frac{Sd32}{R}. \quad (59)$$

The computation time of UBAR is given by

$$T_{\text{UBAR-computation}} = T_{\text{dist-based}} + T_{\text{perf-based}} + T_{\text{agg}} + T_{\text{SGD}}, \quad (60)$$

where  $T_{\text{dist-based}}$ ,  $T_{\text{perf-based}}$ ,  $T_{\text{agg}}$  and  $T_{\text{SGD}}$  are respectively the times to apply the distance-based strategy, the performance-based strategy, the aggregation, and one step of SGD model update. Hence, the total training time when using UBAR for  $K$  training rounds is given by

$$T_{\text{UBAR}} = K(T_{\text{dist-based}} + T_{\text{perf-based}} + T_{\text{agg}} + T_{\text{SGD}} + ST_{\text{comm}}), \quad (61)$$

where  $T_{\text{comm}} = \frac{d32}{R}$ .

## APPENDIX H

In this section, we provide the details of the neural networks used in our experiments, some key details regarding the UBAR implementation, and multiple additional experiments to further demonstrate the superiority of our proposed algorithms. We start in Section H-A by describing the model that is used in our experiments in Section VI and the additional experiments given in this section. In Section H-B, we discuss the implementation of UBAR. After that, we run additional experiments by using MNIST dataset [29] in Section H-C. In Section H-D, we study the computation time of Basil compared to UBAR, and the training performance of Basil and UBAR with respect to the training time. Finally, we study the performance of Basil and ACDS for CIFAR100 dataset with non-IID data distribution in Section H-E, and the performance comparison between Basil and Basil+ in Section H-F.

### A. Models

We provide the details of the neural network architectures used in our experiments. For MNIST, we use a model with three fully connected layers, and the details for the same are provided in Table I. Each of the first two fully connected layers is followed by ReLU, while softmax is used at the output of the third one fully connected layer.

TABLE I  
DETAILS OF THE PARAMETERS IN THE ARCHITECTURE OF THE NEURAL NETWORK USED IN OUR MNIST EXPERIMENTS.

Parameter	Shape
fc1	$784 \times 100$
fc2	$100 \times 100$
fc3	$100 \times 10$

For CIFAR10 experiments in the main paper, we consider a neural network with two convolutional layers, and three fully connected layers, and the specific details of these layers are provided in Table II. ReLU and maxpool is applied on the convolutional layers. The first maxpool has a kernel size  $3 \times 3$  and a stride of 3 and the second maxpool has a kernel size of  $4 \times 4$  and a stride of 4. Each of the first two fully connected layers is followed by ReLU, while softmax is used at the output of the third one fully connected layer.

We initialize all biases to 0. Furthermore, for weights in convolutional layers, we use Glorot uniform initializer, while for weights in fully connected layers, we use the default Pytorch initialization.

TABLE II  
DETAILS OF THE PARAMETERS IN THE ARCHITECTURE OF THE NEURAL NETWORK USED IN OUR CIFAR10 EXPERIMENTS.

Parameter	Shape
conv1	$3 \times 16 \times 3 \times 3$
conv2	$16 \times 64 \times 4 \times 4$
fc1	$64 \times 384$
fc2	$384 \times 192$
fc3	$192 \times 10$

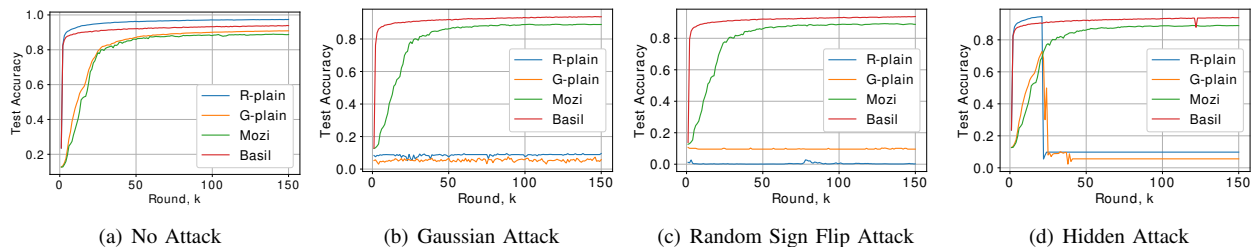


Fig. 10. Illustrating the results for MNIST under IID data distribution setting.

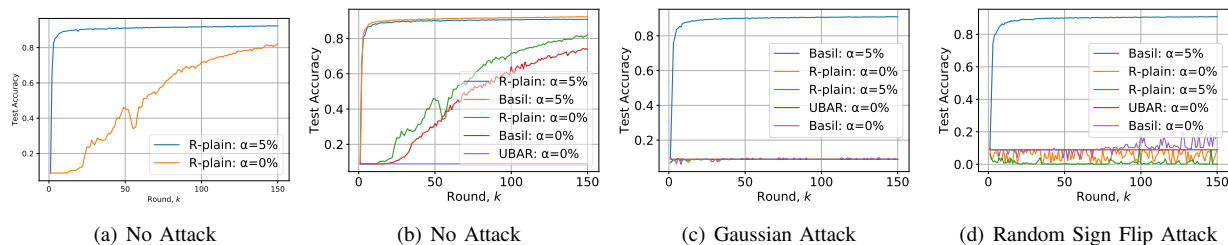


Fig. 11. Illustrating the results for MNIST under non-IID data distribution setting.

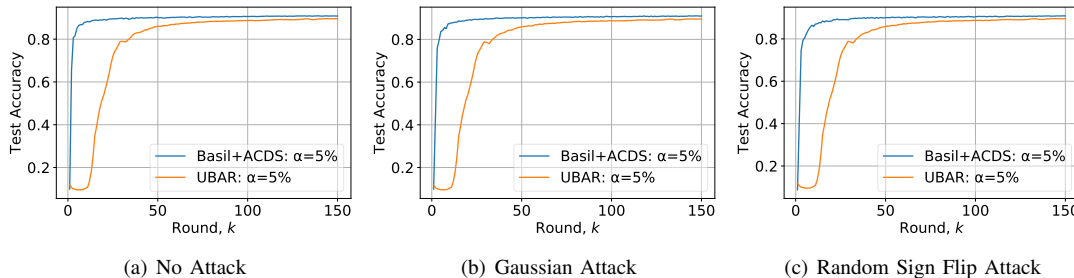


Fig. 12. Illustrating the performance of Basil compared with UBAR for MNIST under non-IID data distribution setting with  $\alpha = 5\%$  data sharing.

## B. Implementing UBAR

We follow a similar approach as described in the experiments in [10]. Specifically, we first assign connections randomly among benign nodes with a probability of 0.4 unless otherwise specified, and then randomly assign connections from the benign nodes to the Byzantine nodes, with a probability of 0.4 unless otherwise specified. Furthermore, we set the Byzantine ratio for benign nodes as  $\rho = 0.33$ .

## C. Performance of Basil on MNIST

We present the results for MNIST in Fig. 10 and Fig. 11 under IID and non-IID data distribution settings, respectively. As can be seen from Fig. 10 and Fig. 11 that using Basil leads to the same conclusions shown in CIFAR10 dataset in the main paper in terms of its fast convergence, high test accuracy, and Byzantine robustness compared to the different schemes. In particular, Fig. 10 under IID data setting demonstrates that Basil is not only resilient to Byzantine attacks, it maintains its superior convergence performance over UBAR. Furthermore, Fig. 10(a) and Fig. 10(b) illustrate that the test accuracy when using Basil and R-plain under non-IID data setting increases when each node shares 5% of its local data with other nodes in the absence of Byzantine nodes. It can

also be seen from Fig. 10(c) and Fig. 10(d) that ACDS with  $\alpha = 5\%$  on the top of Basil provides the same robustness to software/hardware faults represented in Gaussian model and random sign flip as concluded in the main paper. Additionally, we observe that both Basil without ACDS and UBAR completely fail in the presence of these faults.

Similar to the results in Fig. 6 in the main paper, Fig. 12 shows that even 5% data sharing is done in UBAR, performance remains quite low in comparison to Basil+ACDS.

## D. Wall-Clock Time Performance of Basil

In this section, we show the training performance of Basil and UBAR with respect to the training time instead of the number of rounds. To do so, we consider the following setting.

**Experimental setting.** We consider the same setting discussed in Section VI-A in the main paper where there exists a total of 100 nodes, in which 67 are benign. For the dataset, we use CIFAR10. We also consider the Gaussian attack. We set the connectivity parameter for the two algorithms to be  $S = 10$ .

Now, we start by giving the computation/communication time of Basil and UBAR.

**Computation time.** We measured the computation time of Basil and UBAR on a server with AMD EPYC 7502

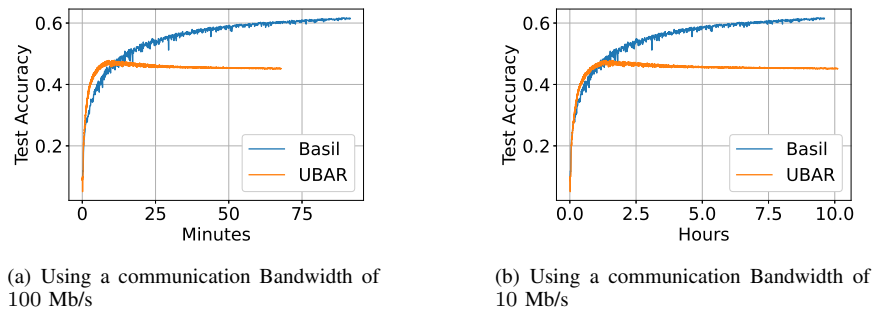


Fig. 13. Illustrating the performance of Basil using CIFAR10 dataset under IID data distribution setting with respect to the training time.

TABLE III  
THE BREAKDOWN OF THE AVERAGE COMPUTATION TIME PER NODE FOR BASIL AND UBAR.

Algorithm	Average evaluation time per node (s)		Aggregation (s) $T_{agg}$	SGD step (s) $T_{SGD}$	Total computation time per node (s)
	Performance-based $T_{per-based}$	Distance-based $T_{dis-based}$			
Basil	0.019	-	-	0.006	0.025
UBAR	0.012	0.027	0.002	0.006	0.047

32-Core CPU Processor. In particular, in TABLE III, we report the average running time of each main component (function) of UBAR and Basil. To do that, we take the average computation time over  $10^3$  runs of each component in the mitigation strategy on each training round for 100 rounds. These functions (components of the mitigation strategy) are the performance-based evaluation for Basil given in Section III, while for UBAR these functions are the performance-based evaluation and the distance-based evaluation along with the model aggregation for UBAR given in Appendix G. We can see from TABLE III that the average time each benign node in UBAR takes to evaluate the received set of models and take one step of model update using SGD is  $\sim 2\times$  the one in Basil. The reason is that each benign node in UBAR performs two extra stages before taking the model update step: (1) distance-based evaluation and (2) model aggregation. The distance-based stage includes a comparison between the model of each benign node and the received set of models which is a time-consuming operation compared to the performance-based as shown in Table III.

**Communication time.** We consider an idealistic simulation, where the communication time of the trained model is proportional to the number of elements of the model. In particular, we simulate the communication time taken to send the model as used in Section VI and described in Appendix H-(B) to be given by  $T_{comm} = \frac{32d}{R}$ , where the model size is given by  $d = 117706$  parameters where each is represented by 32 bits and  $R$  is the bandwidth in Mb/s. To get the training time after  $K$  rounds, we use the per round time result for Basil and UBAR that are given in Proposition 4 in Section VI and Appendix G-(B), respectively, while considering  $K$  to be the number of training rounds.

**Results.** Fig. 13 demonstrates the performance of Basil and UBAR with respect to the training time. As we can observe in Fig. 13, the time it takes for UBAR to reach its maximum accuracy is almost the same as the time for Basil to reach UBAR’s maximum achievable accuracy. We

recall from Section VI that UBAR needs  $5\times$  more computation/communication resources than Basil to get 41% test accuracy. The performance of Basil and UBAR with respect to the training time is not surprising as we know that Basil takes much less training rounds to reach the same accuracy that UBAR can reach as shown in Fig. 4. As a result, the latency resulting from the sequential training does not have high impact in comparison to UBAR. Finally, we can see that the communication time is the bottleneck in this setting as when the BW increases from 10 Mb/s to 100 Mb/s the training time decreases significantly.

#### E. Performance of Basil for Non-IID Data Distribution using CIFAR100

To demonstrate the practicality of ACDS and simulate the scenario where each node shares data only from its non-sensitive dataset portion, we have considered the following experiment.

**Dataset and hyperparameters.** We run image classification task on CIFAR100 dataset [30]. This dataset is similar to CIFAR10 in having the same dimension ( $32 \times 32 \times 3$ ), except it has 100 classes containing 600 images each, where each class has its own feature distribution. There are 500 training images and 100 testing images per class. The 100 classes in the CIFAR100 are grouped into 20 superclasses. For instance, the superclass Fish includes these five subclasses; Aquarium fish, Flatfish, Ray, Shark and Trout. In this experiment, we consider a system of a total of 100 nodes, in which 80 are benign. We have set the connectivity parameter of Basil to  $S = 5$ . We use a decreasing learning rate of  $0.03/(1+0.03k)$ , where  $k$  denotes the training round. For the classification task, we only consider the superclasses as the target labels, i.e., we have 20 labels for our classification task.

**Model architecture.** We use the same neural network that is used for CIFAR10 in the main paper which consists of 2 convolutional layers and 3 fully connected layers, with the

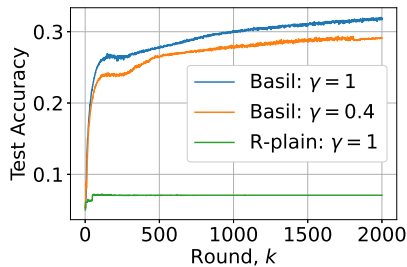


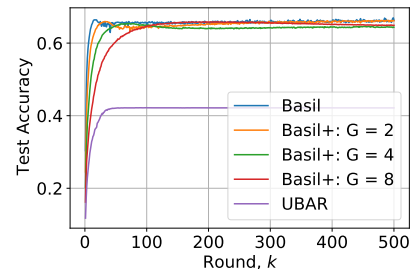
Fig. 14. The performance of `Basil` under different data sharing scenario in the presence of the Gaussian attack when the data distribution at the nodes is non-IID. Here,  $\gamma$  represents the fraction of subclasses that nodes consider the data from them as non-sensitive out of its available 5 subclasses.

modification that the output of the last layer has a dimension of 20. The details for this network are included in Appendix H-A.

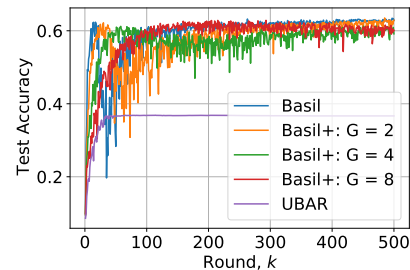
**Data distribution.** For simulating the non-IID setting, we first shuffle the data within each superclass, then partition each superclass into 5 portions, and assign each node one partition. Hence, each node will have only data from one superclass and includes data from each of the corresponding 5 subclasses.

**Data sharing.** To simulate the case where each node shares data from the non-sensitive portion of its local data, we take the advantage of the variation of the feature distribution across subclasses and simulate the sensitive and non-sensitive data as per subclasses. Towards achieving this partition goal, we define  $\gamma \in (0, 1)$  to represent the fraction of subclasses that a node considers their data as non-sensitive out of its available 5 subclasses. For instance,  $\gamma = 1$  implies that all the 5 subclasses are considered non-sensitive and nodes can share data from them (e.g., nodes can share data from their entire local data). On the other hand,  $\gamma = 0.4$  means that all nodes only consider the first two subclasses of their data as non-sensitive and only share data from them. We note that for nodes that share the same superclass, we consider the order of the subclasses are the same among them (e.g., if node 1 and node 2 have data from the same superclass Fish, hence the subclass Aquarium fish is the first subclass at both of them). This ensures that for  $\gamma = 0.4$  data in 3 subclasses per each superclass will never be shared by any user. Finally, we allow each node to share  $\alpha D$  data points, where  $D = 500$  is the local data set size at each node, from the  $\gamma$  subclasses, and  $\alpha = 5\%$ .

**Results** Fig. 14 shows the performance of `Basil` in the presence of the Gaussian attack under different  $\gamma$  values. As we can see that even when each node shares data from only two subclasses ( $\gamma = 0.4$ ) out of the five available subclasses, `Basil` is giving a comparable performance to the case where each node shares data from its entire dataset ( $\gamma = 1$ ). The intuition behinds getting a good performance in the presence of Byzantine nodes is the fact that although data from the three subclasses in each superclass is never shared, there are nodes in the system originally that have data from these sensitive classes, and when they train the model on their local dataset, the augmented side information from the shared dataset helps to maintain the model performance and resiliency to Byzantine faults. Furthermore, we can see that `R-plain` fails



(a) Reporting the average test accuracy among the benign nodes in each round.



(b) Reporting the worst case test accuracy among the benign nodes in each round.

Fig. 15. Illustrating the performance of `Basil` and `Basil+` for CIFAR10 dataset.

in the presence of the attack, demonstrating that the ACDS data sharing is quite crucial for good performance when data is non-IID.

#### F. Performance Comparison Between `Basil` and `Basil+`

We compare the performance of `Basil` and `Basil+` under the following setting:

**Setting.** We consider a setting of 400 nodes in which 80 of them are Byzantine nodes. For the dataset, we use CIFAR10 dataset, while considering inverse attack for the Byzantine nodes. We use a connectivity parameter of  $S = 6$  for both `Basil` and `Basil+`, and consider epoch based local training, where we set the number of epochs to 3.

**Results:** As we can see from Fig. 15, `Basil` and `Basil+` for different groups retain high test accuracy over `UBAR` in the presence of the inverse attack. We can also see from Fig. 15-(b) that when we have a large number of nodes in the system increasing the number of groups (e.g.,  $G = 8$ ) makes the worst case training performance of the benign nodes more stable across the training rounds compared to `Basil` that has high fluctuation for large setting (e.g., 400 nodes).